Journal of Food and Drug Analysis

Volume 31 | Issue 4 Article 11

An integrated strategy to evaluate active substances of Astragali Radix-Carthami Flos combination on the treatment of cerebral ischemia reperfusion injury based on TQSM polypharmacokinetics and pharmacodynamics

ORIGINAL ARTICLE

An integrated strategy to evaluate active substances of Astragali Radix-Carthami Flos combination on the treatment of cerebral ischemia reperfusion injury based on TQSM polypharmacokinetics and pharmacodynamics

Qiang Zeng [a], Chang Li [b], Shouchao Xu [a], Yu He [a,*]

[a] School of Pharmaceutical Sciences, Zhejiang Chinese Medical University, Hangzhou 310053, PR China
[b] School of Life Sciences, Zhejiang Chinese Medical University, Hangzhou 310053, PR China

Abstract

As a classic herb pair, Astragali Radix-Carthami Flos (AR-CF) has revealed good biological activity in the treatment of cerebral ischemia/reperfusion injury (CI/RI), which remained to be further clarified together with the underlying efficacy related compounds for material basis. In this study, the nine formulations were obtained by L_9 (3^4) orthogonal array design of four active fractions (saponin and flavonoid extracted from AR, safflower yellow and safflower red extracted from CF). The concentrations of eleven components and the levels of four biochemical indicators in rat plasma were continuously detected after intragastric administration of nine formulations, respectively. The collected data were analyzed by sigmoid-E_{max} function to understand the polypharmacokinetics and pharmacodynamics (PK-PD) behaviors of multi-components. Using the total quantum statistic moment polypharmacokinetics and its similarity method, the importance of four active fractions from AR-CF in relieving CI/RI was discussed and the Q-markers were screened. The results represented that a reliable and robust liquid chromatography tandem mass spectrometry method been successfully established to simultaneously determine the concentrations of eleven components in rat plasma. The AUC and MRT values of components from flavonoid fraction had the greatest contribution to AUC_T and MRT_T values. The transitivity *in vivo* of calycosin-7-*O*-*β*-D-glucoside (CG), astragaloside IV (AIV) and hydroxysafflor yellow A (HYA) was closer to polypharmacokinetics behavior. All formulations up/down-regulated the levels of GSH-Px and ATP/ET and LDH to varying degrees, among which formulation 7 had the best regulating effect. By drawing the time-concentration-effect curve, clockwise hysteresis loops were presented in the time-concentration-effect relationships between eleven components and LDH/ET, while the relationship between eleven components and ATP/GSH-Px expressed as anticlockwise hysteresis loops. In conclusion, the combination based on the combination principle of formulation 7 produced the best alleviation effect on CI/RI, and flavonoid fraction might played key role in this process. The CG, AIV and HYA were identified as Q-markers. This research offered a novel strategy for exploring the active substances, and provided further understanding regarding the development of drugs for the treatment of cerebral ischemia-reperfusion injury.

Keywords: Active substances, Astragali Radix, Carthami Flos, Cerebral ischemia/reperfusion injury, Pharmacokineticspharmacodynamics

Abbreviations: AIC, Akaike Information Criterion; AIII, astragaloside III; AIV, astragaloside IV; ATP, Adenosine triphosphate; AR-CF, Astragali Radix-Carthami Flos; AUC, area under the curve; BIC, Bayesian Information Criterion; CG, calycosin-7-*O*-*β*-D-glucoside; HPLC, High performance liquid chromatography; AYB, anhydrosafflor yellow B; CAL, Calycosin; CAR, carthamin; CI/RI, cerebral ischemia/reperfusion injury; CVD, cardiovascular diseases; DG, 9,10-dimethoxyptercarpan-3-*O*-*β*-D-glucoside; ET, endothelin; FOR, formononetin; GSH-Px, glutathione peroxidase; HYA, hydroxysafflor yellow A; IG, isomucronulatol 7-*O*-glucoside; ISs, internal standards; MRT, mean residence time; LDH, lactate dehydrogenase; LLOQ, lower limit of quantification; MRM, multiple reaction monitoring; MCAO/R, Middle cerebral artery occlusion/reperfusion; ONO, ononin; TCM, Traditional Chinese Medicine; PD, pharmacodynamics; PK, pharmacokinetics; QCs, quality control samples; TQSM, total quantum statistic moment; LC-MS/MS, liquid chromatography tandem mass spectrometry.

Received 23 May 2023; accepted 5 September 2023.
Available online 15 December 2023

* Corresponding author.
E-mail address: heyu092@hotmail.com (Y. He).

https://doi.org/10.38212/2224-6614.3477

1. Introduction

Cardiovascular diseases (CVD) such as stroke, heart attack and primary hypertension are the leading cause of death globally, among which stroke, especially ischemic stroke, accounts for a large proportion of CVD mortality [1]. The main treatment method for ischemic stroke is reperfusion treatment based on thrombolytic and thrombectomy. However, as one of the most serious complications, cerebral ischemia/reperfusion injury (CI/RI) may occur after revascularization [2]. An accumulating body of research has reported that CI/RI hindered post-stroke recovery through various complex pathological mechanisms, for example, apoptosis, oxidative stress, inflammation, etc. [3–5]. Consequently, it is pressing to discover safer and more effective alternative treatments in alleviating the CI/RI to manage ischemic stroke.

For thousands of years, Traditional Chinese Medicine (TCM) has been used to prevent and treat many diseases, with well clinical therapeutic effects and low incidence of adverse events. It has been incorporated into the ancient medical system as a therapy for various stroke-related diseases [6–8]. As a classic herb pair, Astragali Radix (AR)-Carthami Flos (CF) is the core of many TCM formulas for treating CI/RI, and has good clinical efficacy in alleviating CI/RI [9–12]. In addition, active fractions extracted from AR and CF also alleviate CI/RI through different regulatory pathways. For example, saponin and flavonoid extracted from AR improved CI/RI by exerting antioxidant activity, safflower yellow and safflower red extracted from CF alleviated the production of free radicals and inflammation during CI [10,12,13]. Therefore, these four fractions were also regarded as the important active fractions of AR-CF [14,15]. It is difficult to generalize the overall effect of the prescription by studying the efficacy of individual fraction. Effective combination composed of multiple fractions reflect the characteristics of multi-components and multi-target therapy of TCM or prescription. By comparing the efficacy of combinations of active fractions under different compatibility ratios, we understand the core in compatibility and synergism of active fractions of prescription. The compatibility of the four fractions from AR-CF has not been explored in terms of pharmacological effects.

Pharmacokinetics (PK) has become a potent means to explain the synergistic mechanism of TCM by reflecting the dynamic changes of active materials *in vivo* [16]. In previous researches, the PK of multiple components in the AR or CF has mostly been reported, but not in the combinations of active fractions from AR-CF. Furthermore, the dynamic correlations between the multicomponents PK and pharmacological effects of the combination of active fraction from AR-CF remain unclear. Pharmacokinetics-Pharmacodynamics (PK-PD) modeling is an efficient method to dynamically correlate the concentration-time courses and effect-time profiles [17]. As a viable approach to elucidate the synergism of a formula's multiple components, it has been applied widely for drug screening, dosing regimen selection and clinical trial design [18]. Therefore, based on the PK of multi-components in rat plasma and the pharmacological effects of the combination of active fraction from AR-CF on CI/RI, the correlation between the PK of multi-components and the PD over time may be explored by PK-PD modeling. As a viable method, PK-PD modeling will be used in this experiment to elucidate the therapeutic material basis and effects of AR-CF.

The total quantum statistic moment (TQSM) polypharmacokinetics, which is similar to describing and comparing the pharmacokinetic behaviors of multi-components, is a feasible method to screening TCM quality marker (Q-marker). By analyzing the statistical moment properties of Q-marker candidates in the TQSM polypharmacokinetic model, the appropriate Q-markers in TCM were screened out. The structures of calycosin (CAL), calycosin-7-*O*-β-D-glucoside (CG), astragaloside III (AIII), formononetin (FOR), ononin (ONO), astragaloside IV (AIV), isomucronulatol 7-*O*-glucoside (IG), 9,10-dimethoxyptercarpan-3-*O*-β-D-glucoside (DG), hydroxysafflor yellow A (HYA), anhydrosafflor yellow B (AYB) and carthamin (CAR) were shown in Fig. 1, which were considered as the important Q-marker candidates in AF-CF. CAL, CG, FOR, ONO, IG and DG were derived from flavonoid, while AIII and AIV were derived from saponin, all of which have good biological activities, especially CG and AIV. CG and AIV were the markers of quality evaluation in Chinese Pharmacopoeia [11,19]. HYA and AYB were derived from safflower yellow, while CAR was derived from safflower red. In CF, HYA and AYB were the two most abundant water-soluble components, while CAR was the representative fat-soluble component. It was reported that HYA, AYB and CAR have great potential in the prevention and treatment of CVD [20–22].

In this study, the nine formulations were obtained by L_9 (3^4) orthogonal array design of four active fractions (saponin and flavonoid extracted from AR, and safflower yellow and safflower red extracted from CF). A liquid chromatography

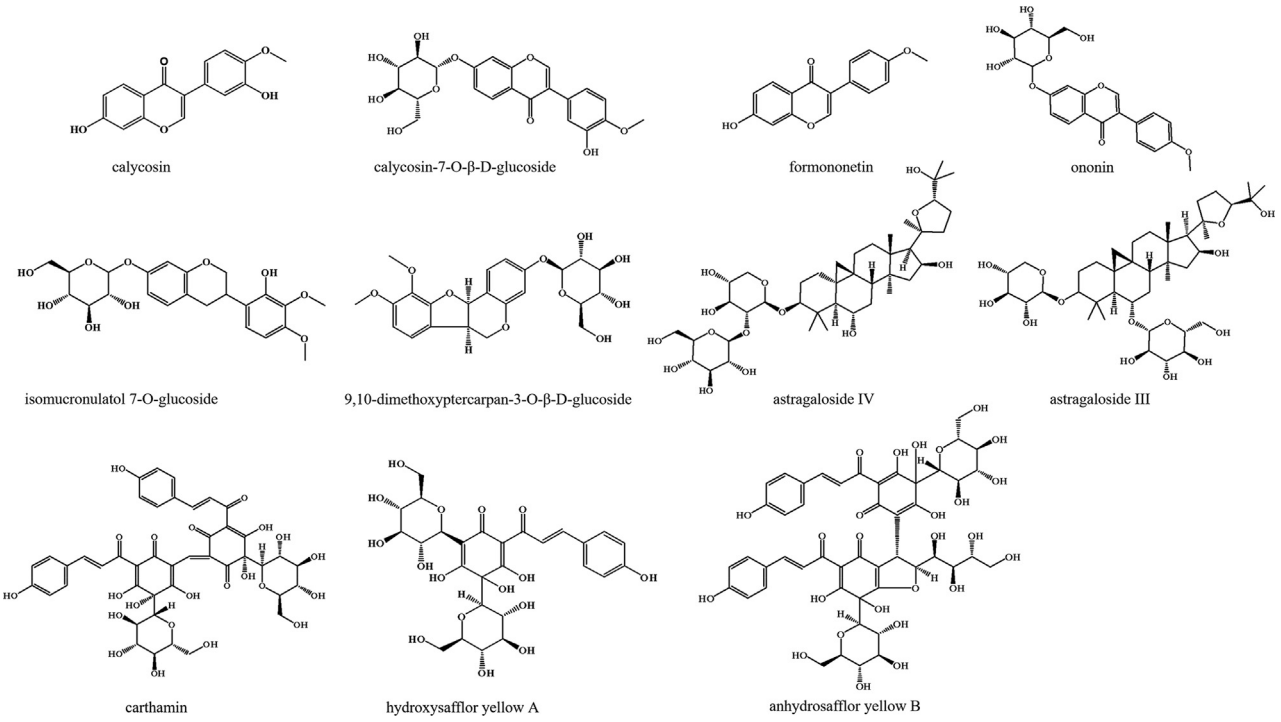

Fig. 1. Chemical structure of eleven components.

tandem mass spectrometry method (LC-MS/MS) was exploited to determine the concentrations of the above eleven Q-marker candidates in middle cerebral artery occlusion/reperfusion (MCAO/R) rat after respectively intragastric administration of nine formulations. Moreover, the levels of adenosine triphosphate (ATP), glutathione peroxidase (GSH-Px), lactate dehydrogenase (LDH) and endothelin (ET) in rat plasma were measured to evaluate the effect of nine formulations on CI/RI. The Q-markers and roles of active fractions for the anti-CI/RI effect of AR-CF were determined after using the TQSM polypharmacokinetics and its similarity approach to analyze the transportability *in vivo* of eleven candidates. Finally, based on the integration of measurable PK components and biochemical indicators, a PK-PD model was constructed to understand the PK-PD behaviors of multi-components from AR-CF in MCAO/R rats.

2. Materials and methods

2.1. Material and reagents

Astragali Radix (dried root of Leguminous plant *Astragalus membranaceus* (Fisch.) Bge., batch number: 20210818) and Carthami Flos (dried flowers of Compositae plant *Carthamus tinctorius* L., batch number: 20210806) were purchased from Hangzhou Huadong Herbal Pieces Co., Ltd. (Zhejiang, China), and authenticated by Professor Shengwu Huang of Zhejiang Chinese Medical University.

The standards of HYA (batch number: DSTDQ001702), CAL (batch number: DST200609-012), CG (batch number: DST200619-013), AIII (batch number: DST201116-023), FOR (batch number: DST191202-011), ONO (batch number: DST201129-044), AIV (batch number: DSTDH001501), DG (batch number: DST200206-159), IG (batch number: DST200629-107) and puerarin (batch number: DSTDG000201) were purchased from Chengdu Dester Technology Co., Ltd (Chengdu, China), digoxin (batch number: 0222-RA-0003) was purchased from CATO Research Chemicals Inc. (Guangzhou, China), nimodipine (batch number: H10910081) was purchased from Shandong Xinhua Pharmaceutical Co., Ltd (Shandong, China), AYB and CAR were prepared as described in our previous study [23,24]. The purity of all standards was greater than or equal to 98%.

Enzyme linked immunosorbent assay (ELISA) kits, including ATP kit (MB-6931A), GSH-Px kit (MB-6722A), LDH kit (MB-6863A) and ET kit (MB-6634A), were purchased from Jiangsu Mei Biao Biological Technology Co., Ltd. (Jiangsu, China).

2.2. Preparation of herbal active fractions

Saponin fraction and flavonoid fraction from AR, and safflower yellow fraction and safflower red

fraction from CF were prepared according to the methods previously reported in our laboratory [23–26]. Meanwhile, CG (49.5 μg/mg), CAL (9.4 μg/mg), FOR (1.3 μg/mg), IG (9.9 μg/mg), ONO (11.2 μg/mg) and DG (3.9 μg/mg) from flavonoid fraction, AIII (47.1 μg/mg) and AIV (105.8 μg/mg) from saponin fraction, AYB (50.6 μg/mg) and HYA (304.8 μg/mg) from safflower yellow fraction, and CAR (63.8 μg/mg) from safflower red fraction were found and identified. The representative HPLC was shown in Suppl. Fig. 1 and the detailed preparation processes for four fractions were described in the supplement material.

2.3. LC-MS/MS analysis

The chromatographic conditions were optimized through OSAKA SODA CAPCELL PAK ADME HR C_{18} Column (3 μm, 4.6 mm × 150 mm). 0.1% aqueous formic acid (A) and acetonitrile (B) made up the mobile phase. The following were the gradient elution conditions: 0–2 min, B from 10% to 31%, 2–6 min, B from 31% to 45%, 6–26 min, B from 45% to 52%, 26–27 min, B from 52% to 95%, 27–29 min, maintain 95%, 29–30 min, B from 95% to 10%. The flow rate of 0.5 mL/min and injection volume of 5 μL were used.

Mass spectrometric detection was operated on mass spectrometer (API 4500 Q-TRAP, AB SCIEX, USA) in multiple reaction monitoring (MRM) mode. The source temperature, curtain gas (nitrogen), heater gas (nitrogen) and nebulizer gas (nitrogen) were 500 °C, 30 psi, 50 psi and 50 psi, respectively. AYB, CAL, HYA, CAR and puerarin were monitored in negative ionization mode with −4500 V, other analytes were monitored in positive ionization mode with 5000 V. Some other MS parameters were shown in Suppl. Table 1.

2.4. Samples preparation

Accurately weighed standards were dissolved with methanol to prepare stock solutions consisting of 1.43 mg/mL for CAL, 2.02 mg/mL for CG, 2.26 mg/mL for FOR, 2.36 mg/mL for ONO, 0.95 mg/mL for IG, 0.61 mg/mL for DG, 0.98 mg/mL for AIV, 0.65 mg/mL for AIII, 4.90 mg/mL for AYB, 2.64 mg/mL for HYA and 0.52 mg/mL for CAR. Individual stock solutions were serially diluted before being blended together to create working standard solutions. The calibration standard solutions were prepared by adding mixed working solution to blank plasma.

Quality control samples (QCs) were prepared similarly at 3.5, 10.5, 100, 6000 ng/mL for CG, 0.5, 1.5, 100, 2000 ng/mL for CAL, 1, 3, 100, 2000 ng/mL for ONO, 8, 24, 100, 2000 ng/mL for FOR, 1, 3, 100, 2000 ng/mL for IG, 10, 30, 100, 2000 ng/mL for DG, 5, 15, 100, 4000 ng/mL for AIV, 10, 30, 100, 2000 ng/mL for AIII, 8, 24, 2000, 30000 ng/mL for HYA, 50, 150, 2000, 20000 ng/mL for AYB, 50, 150, 2000, 10000 ng/mL for CAR, respectively. The concentrations of internal standard (IS) solutions were 100 ng/mL (puerarin) and 1000 ng/mL (digoxin).

2.5. Plasma sample pretreatment

20 μL puerarin, 20 μL digoxin, 100 μL rat plasma and 360 μL methanol were added to an empty tube, followed by fully vortex mixing for 3 min. Afterward, the mixed samples were centrifuged at 12000 rpm for 10 min at 4 °C. The supernatant was transferred to new tube and blown dry under mild nitrogen. The residue was redissolved with 100 μL injection solvent (mixture of mobile phase A and B, 90/10, v/v), and centrifuged at 12000 rpm for 10 min at 4 °C. The processed samples were stored at −20 °C.

2.6. Method validation

According to relevant guidelines, the calibration standards and QCs were applied to validate the specificity, precision, accuracy, linearity, stability, matrix effect and recovery of the analytical method [27].

2.7. Experimental design

The experimental animals were Sprague–Dawley male rats, which were supplied from the Zhejiang Chinese Medical University Laboratory Animal Research Center. Rats were raised in SPF laboratory conditions and free diet prior to experimental use. The rats (280–320 g) were acclimated to the feeding conditions for at least one week. The "Guiding Principles in the Care and Use of Animals" (China) were followed for conducting the animal study, which received approbation from the Animal Subjects Review Board of Zhejiang Chinese Medical University (approval number: SYXK (Zhe) 2021-0012).

Rats were randomly divided into twelve groups (a sham-operation group, a model group, a positive drug group and nine model treated groups, n = 6 each group) and fasted 12 h before the experiment. Nimodipine, a widely reported anti-CI/RI drug, was used as positive drug in this study [28,29]. The transient MCAO approach with suitable modification was used to induce the focal CI/RI model

[30,31]. After a brief MCAO for 1 h, the monofilament was slowly withdrawn and rats were kept under a warming lamp during the operation until woke up.

All administration doses were exhibited in milligrams of each active fraction per kilogram of body weight (mg/kg). The dose was founded on body weight measured prior to dosing. The ratio of Astragali Radix (AR) to Carthami Flos (CF) in the AR-CF was determined as 3:1 (weight:weight) based on the previous research results and the ratio of AR to CF in TCM prescription [3]. According to the Chinese Pharmacopoeia (2020 edition) [32], the recommended clinical doses for adults were 30 g/day for AR and 10 g/day for CF. Based on pilot experiments, three dose levels of AR and CF were defined, which were 2 times, 4 times, and 8 times the clinical equivalent doses, respectively. After obtaining the yield of the four fractions, the three dose levels of four fractions extracted from AR-CF were determined through the conversion of yield, respectively. The L_9 (3^4) orthogonal table was used to design nine formulations. The orthogonal design scheme was composed of four-factors (four fractions) and three-levels (three dose levels). The combination scheme of nine formulations were shown in Table 1. Positive drug group rats were given 14.4 mg/kg nimodipine, other two groups rats were given the same amount of saline intragastrically.

About 0.5 mL blood sample was collected from rat fossa orbitalis vein into vacuum tubes containing heparin sodium anticoagulant at 0.083, 0.25, 0.5, 0.75, 1, 2, 3, 4, 6, 8, 12, 24 h respectively after dosing. Collected blood was immediately replaced with equal volume of sterile normal saline by intraperitoneal injection. The blood samples that were gathered underwent centrifugation, and the resulting supernatants were harvested and kept at a temperature of −20 °C. Two parts were obtained by dividing the supernatant, the first part containing 100 μL supernatant was pretreated according to the plasma sample pretreatment method, and the concentrations of eleven components were detected according to the established LC-MS/MS approach; the remaining supernatant was used to measure the LDH, ATP, GSH-Px and ET levels by ELISA according to the respective manufacturers' guidelines.

2.8. PK and PD modeling

The contents of LDH, ATP, GSH-Px and ET were applied to calculate treatment-related changes to facilitate PK-PD simulations using the following equation:

$$|\Delta LDH_T - \Delta LDH_M| = |(LDH_{Tt} - LDH_{T0}) - (LDH_{Mt} - LDH_{M0})| \quad (1)$$

where ΔLDH_T and ΔLDH_M meant the change of LDH values in treatment groups and model group, respectively. LDH_{Tt} and LDH_{Mt} meant the levels of LDH at time t in treatment groups and model group, respectively. LDH_{T0} and LDH_{M0} meant the baseline LDH levels in treatment groups and model group, respectively. The equations of ATP, GSH-Px and ET were the same as above.

Plasma levels of four pharmacodynamic indicators and concentrations of eleven components were applied to formulate the PK-PD relationship model. The sigmoid E_{max} was chosen for PK-PD analysis because the best goodness of fit values was obtained when using the following equation [33]:

$$E = \frac{E_{max} \times C^{\gamma}}{EC_{50}^{\gamma} + C^{\gamma}} \quad (2)$$

where E, E_{max}, EC_{50}, C and γ corresponded to the change of pharmacodynamic index levels in plasma, maximal possible efficacy, concentration that achieves 50% of the maximal possible effect, concentration in effect compartment and Hill coefficient, respectively.

Table 1. Dose compatibility of four active fractions of AR-CF.

Formulation	Doses			
	Flavonoid fraction (mg/kg)	Saponin fraction (mg/kg)	Safflower yellow fraction (mg/kg)	Safflower red fraction (mg/kg)
1	120	110	170	240
2	120	220	340	480
3	120	440	680	960
4	240	110	340	960
5	240	220	680	240
6	240	440	170	480
7	480	110	680	480
8	480	220	170	960
9	480	440	340	240

2.9. Statistical data analysis

DAS 3.2.6 is capable of conducting various statistical analyses on drug data, including pharmacokinetic-pharmacodynamic modeling, drug metabolism, drug interaction, and more. It enables fitting of various models, including the sigmoid E_{max} model, and directly generate results for submission. The pharmacokinetic parameters were obtained by DAS 3.2.6 using non-compartmental. Difference in means between two groups was tested using t test. For multiple comparisons of means involving a combination of two or three independent factors, two- or three-way analysis of variance (ANOVA) was performed respectively, followed by Tukey's (to compare all pairs of means) or Holm-Sidak (to compare selected pairs of means) post hoc tests was performed. Statistical analysis was implemented using GraphPad Prism 8.0, with a threshold of $p < 0.05$ for determining statistical significance.

The TQSM parameters of eleven components from nine formulations were respectively calculated using the following equations:

$$AUC_T = \sum_{i=1}^{n} AUC_i \tag{3}$$

$$MRT_T = \frac{\sum_{i=1}^{n}(MRT_i \times AUC_i)}{\sum_{i=1}^{n} AUC_i} \tag{4}$$

where AUC_T (zero moment of total quanta) meant the area under the curve of all components blood concentration versus time (all components concentrations integration versus time from zero to infinite), MRT_T (first moment of total quanta) corresponded to the average retention time for all-components, AUC_i and MRT_i meant the area under curve of *i*th component and the mean residence time of *i*th component, respectively.

The similarity of TQSM (S_T) for two pharmacokinetic profiles was defined to their overlapped area of cross-curve which were converted probability density function surrounding with t-axis. The S_T was calculated using the following equation:

$$S_T = 1 - \left| \int_{t_1}^{t_2} \left[1/\left((2\pi)^{1/2}\cdot\sigma_\alpha\right)\right] \cdot \exp\left[-(t-\bar{t}_\alpha)^2/2\sigma_\alpha^2\right] dt - \int_{t_1}^{t_2} \left[1/\left((2\pi)^{1/2}\cdot\sigma_b\right)\right] \cdot exp\left[-(t-\bar{t}_b)^2/2\sigma_b^2\right] dt \right| \tag{5}$$

The $\bar{t}_\alpha$ and $\bar{t}_b$ were first moment of total quanta for two pharmacokinetic profiles, the σ_α^2 and σ_b^2 were second moment of total quanta for two pharmacokinetic profiles, the cross points for two normal distribution curves were presented both of t_1 and t_2. Detailed descriptions of the above equations were available in the reported literature [34].

3. Results

3.1. Method validation

The mass spectrum chromatograms were presented in Suppl. Fig. 2. MRM mode detected analytes and ISs with high specificity and selectivity. The calibration curves and LLOQ of analytes were shown in Suppl. Table 2. The test ranges of calibration curve fully met the observed concentration and showed good linearity ($R^2 > 0.99$).

The precision and accuracy results of analytes at three QC levels and LLOQ were displayed in Suppl. Table 3. The precision (RSD%) and accuracy (RE%) of intra- and inter-day were less than 15%.

The stability of sample under different storage at three QCs levels was measured. For Suppl. Table 4, the samples were stable under different storage conditions (RSD% < 15%).

As shown in Suppl. Table 5, The matrix effects of analytes were all lower than 15%, and extraction recoveries were all more than 77.0% at three QCs levels. The results suggested that the matrix effect was insignificant on the quantification of analytes.

The results of all methodological investigations met the requirements of the guidelines, suggesting that the established method was appropriate for PK analysis of eleven components.

3.2. TQSM polypharmacokinetics and its similarity analysis

The concentration-time curves of eleven components were displayed in Fig. 2. The corresponding pharmacokinetic parameters for eleven components in nine formulations were listed in Suppl. Table 6-16, the eleven components were quickly absorbed and reached T_{max} between 0.10 and 3.0 h after being administered. Among the nine formulations, the contents of flavonoid fraction in the formulation 1, 2 and 3 were the same. Interestingly, when combined with other fractions in different doses, the pharmacokinetic parameters of the flavonoid from AR in the three formulations were changed, in which the AUC of flavonoid from AR (as a whole) raised with the doses increase of saponin, safflower yellow and safflower red fraction ($p < 0.05$). In addition, the MRT of flavonoid from AR in formulation 2 and 3

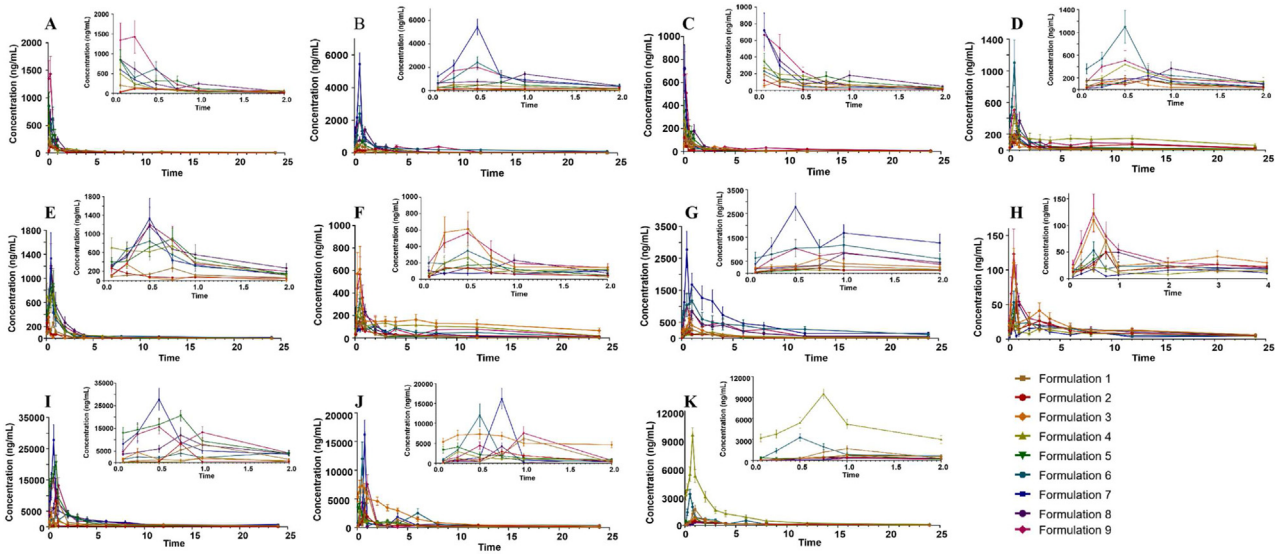

Fig. 2. The mean concentration-time curves of eleven components. (A) calycosin; (B) calycosin-7-O-β-D-glucoside; (C) formononetin; (D) ononin; (E) isomucronulatol 7-O-glucoside; (F) 9,10-dimethoxyptercarpan-3-O-β-D-glucoside; (G) astragaloside IV; (H) astragaloside III; (I) hydroxysafflor yellow A; (J) anhydrosafflor yellow B; (K) carthamin. (Mean ± SD, n = 6).

was larger than that in formulation 1, while the MRT of flavonoid from AR in formulation 2 was not different from that in formulation 3. The results indicated that the AUC of flavonoid from AR would raise with the dose of other fraction, but the MRT would not raise continuously with the dose increase, and it would reach a peak and maintain a relatively stable level (Suppl. Fig. 3). Similarly, the contents of saponin fraction in the formulation 1, 4 and 5 were the same, the contents of safflower yellow fraction in the formulation 1, 6 and 8 were the same, and the contents of safflower red fraction in the formulation 1, 5 and 9 were the same. However, after combining with other fractions of different doses, the pharmacokinetic parameters of representative components in the three formulations with same fraction contents were also different. The results indicated that the different combinations of effective fractions affected the pharmacokinetic prosesses of components *in vivo*.

The TQSM is a statistical analysis method which uses the principle of statistical moment to analyze the continuous or discrete variable function curve and obtain the moment parameters of the whole function. Based on the pharmacokinetic parameters of eleven components in the nine formulations, the TQSM parameters such as AUC_T and MRT_T of eleven components from nine formulations were respectively obtained according to equations (3) and (4). The AUC_T and MRT_T values of eleven components from formulations 1 to 9 were listed in Table 2. The orthogonal design assistant V3.1 was used to conduct variance analysis on the TQSM parameters. A larger *F* value indicates a greater effect of the factor on the results. As shown in Table 3, the effect of flavonoid from AR on AUC_T was statistically significant ($p < 0.05$). The contribution rates of flavonoid, saponin, safflower yellow and safflower red to AUC_T and MRT_T values were 52.09%, 22.15%, 23.90%, 1.86% and 34.14%, 11.77%, 27.27%, 26.82%, respectively. Flavonoid from AR had the greatest contribution to the AUC_T and MRT_T values, suggesting that it may be the main active fraction of AR-CF.

The TQSM pharmacokinetic parameters of eleven components from the formulation 7 were converted into normal distribution probability density function, and each TQSM similarity was calculated out by equation (5). As shown in Table 4, the TQSM similarities (S_T) between the eleven components and their TQSM were 0.8915 (CAL), 0.9067 (CG), 0.7218 (FOR), 0.8905 (ONO), 0.8858 (IG), 0.8612 (DG), 0.9166 (AIV), 0.8930 (AIII), 0.9558 (HYA), 0.8854 (AYB) and 0.8938 (CAR), respectively. The greater value of S_T, the closer pharmacokinetic behavior of the component with the multipharmacokinetic behavior, and the more important role it plays in the multi-component formulations. The S_T values of CG (0.9067), AIV (0.9166) and HYA (0.9558) were all greater than 0.9020.

Table 2. The results of TQSM analysis in nine formulations. (Mean ± SD, n = 6).

Formulation	AUC_T/(μg/L*h)	MRT_T/h
1	42990.81 ± 3362.93	6.87 ± 0.92
2	25541.23 ± 1930.04	6.84 ± 0.59
3	59286.99 ± 4633.36	6.28 ± 0.45
4	47860.77 ± 3012.63	6.16 ± 0.66
5	52107.74 ± 3360.81	3.80 ± 0.40
6	65175.80 ± 5850.49	6.65 ± 0.65
7	87070.78 ± 5176.39	5.66 ± 0.51
8	59744.75 ± 4589.71	5.75 ± 0.69
9	66799.88 ± 4610.41	5.03 ± 0.91

3.3. PD analysis

The LDH, ATP, GSH-Px and ET were monitored by using ELISA at different time points. For Fig. 3A, the contents of LDH, ATP, GSH-Px and ET remained basically stable in sham-operation group and decreased in model group. There were noticeable differences between model group and sham-operation group when analyzing the LDH, ATP, GSH-Px, and ET levels between the two groups, suggesting that the experimental model has been successfully prepared. Furthermore, the contents of LDH and ET in all treatment groups decreased, while the contents of ATP and GSH-Px increased. There were significant differences at most time points during the test ($p < 0.05$).

In terms of the overall trend, AR-CF remarkably reduced the levels of ET and LDH *in vivo* between 3 and 8 h and effectively promoted the generation of ATP between 1 and 4 h after administration. As the active components were metabolized *in vivo*, these regulatory effects were gradually weakened. Interestingly, the regulation effect of AR-CF on GSH-Px release did not decrease with the extension of time. In addition, compared with other formulations, formulation 7 showed significant adjustment ability to the four biochemical indicators at multiple time points within the detection range. The differences among the groups were shown in Fig. 3B through the calculation of AUCs from 0 to 24 h after MCAO/R. It is displayed that the levels of LDH, ET, ATP and GSH-Px of MCAO rats treated with nine formulations were suppressed/promoted in varying degrees. Among the nine formulations, formulation

Table 3. The result of variance analysis of orthogonal test. (n = 6).

Index	Source of variation	Sum of squares	Degrees of freedom	*F* value	Significance	Contribution rate %
AUC_T	Flavonoid	1233738127.99	2	28.03	$p < 0.05$	52.09
	Saponin	524710928.85	2	11.92		22.15
	Safflower yellow	566224680.28	2	12.86		23.90
	Safflower red	44013427.50	2	1.00		1.86
MRT_T	Flavonoid	2.68	2	2.90		34.14
	Saponin	0.92	2	1.00		11.77
	Safflower yellow	2.14	2	2.32		27.27
	Safflower red	2.11	2	2.28		26.82

Note: $F_{0.05,\ (2,2)} = 19$; $F_{0.01,\ (2,2)} = 99$.

Table 4. TQSM similarities of single component and eleven entirety in the formulation 7. (n = 6).

Components	CAL	CG	FOR	ONO	IG	DG	AIV	AIII	HYA	AYB	CAR	TQSM
CAL	1	0.8371	0.7329	0.9512	0.9985	0.9653	0.8123	0.7896	0.8494	0.9857	0.9859	0.8915
CG	0.8371	1	0.8230	0.8009	0.8363	0.8131	0.8222	0.8078	0.8567	0.8376	0.8167	0.9067
FOR	0.7329	0.8230	1	0.8603	0.8192	0.9631	0.6573	0.6310	0.6909	0.8168	0.8140	0.7218
ONO	0.9512	0.8009	0.8603	1	0.9818	0.9530	0.8196	0.8085	0.8521	0.9786	0.9952	0.8905
IG	0.9985	0.8363	0.8192	0.9818	1	0.9678	0.8064	0.7826	0.8442	0.9732	0.9756	0.8858
DG	0.9653	0.8131	0.9631	0.9530	0.9678	1	0.7829	0.7593	0.8196	0.9633	0.9580	0.8612
AIV	0.8123	0.8222	0.6573	0.8196	0.8064	0.7829	1	0.9329	0.9597	0.8025	0.8157	0.9166
AIII	0.7896	0.8078	0.6310	0.8085	0.7826	0.7593	0.9329	1	0.9528	0.7834	0.7988	0.8930
HYA	0.8494	0.8567	0.6909	0.8521	0.8442	0.8196	0.9597	0.9528	1	0.8399	0.8499	0.9558
AYB	0.9857	0.8376	0.8168	0.9786	0.9732	0.9633	0.8025	0.7834	0.8399	1	0.9523	0.8854
CAR	0.9859	0.8167	0.8140	0.9952	0.9756	0.9580	0.8157	0.7988	0.8499	0.9523	1	0.8938
TQSM	0.8915	0.9067	0.7218	0.8905	0.8858	0.8612	0.9166	0.8930	0.9558	0.8854	0.8938	1

Note: The number represents the TQSM similarity for two pharmacokinetic profiles. CAL, calycosin; CG, calycosin-7-*O*-*β*-D-glucoside; FOR, formononetin; ONO, ononin; IG, isomucronulatol 7-*O*-glucoside; DG, 9,10-dimethoxyptercarpan-3-*O*-*β*-D-glucoside; AIV, astragaloside IV; AIII, astragaloside III; HYA, hydroxysafflor yellow A; AYB, anhydrosafflor yellow B; CAR, carthamin.

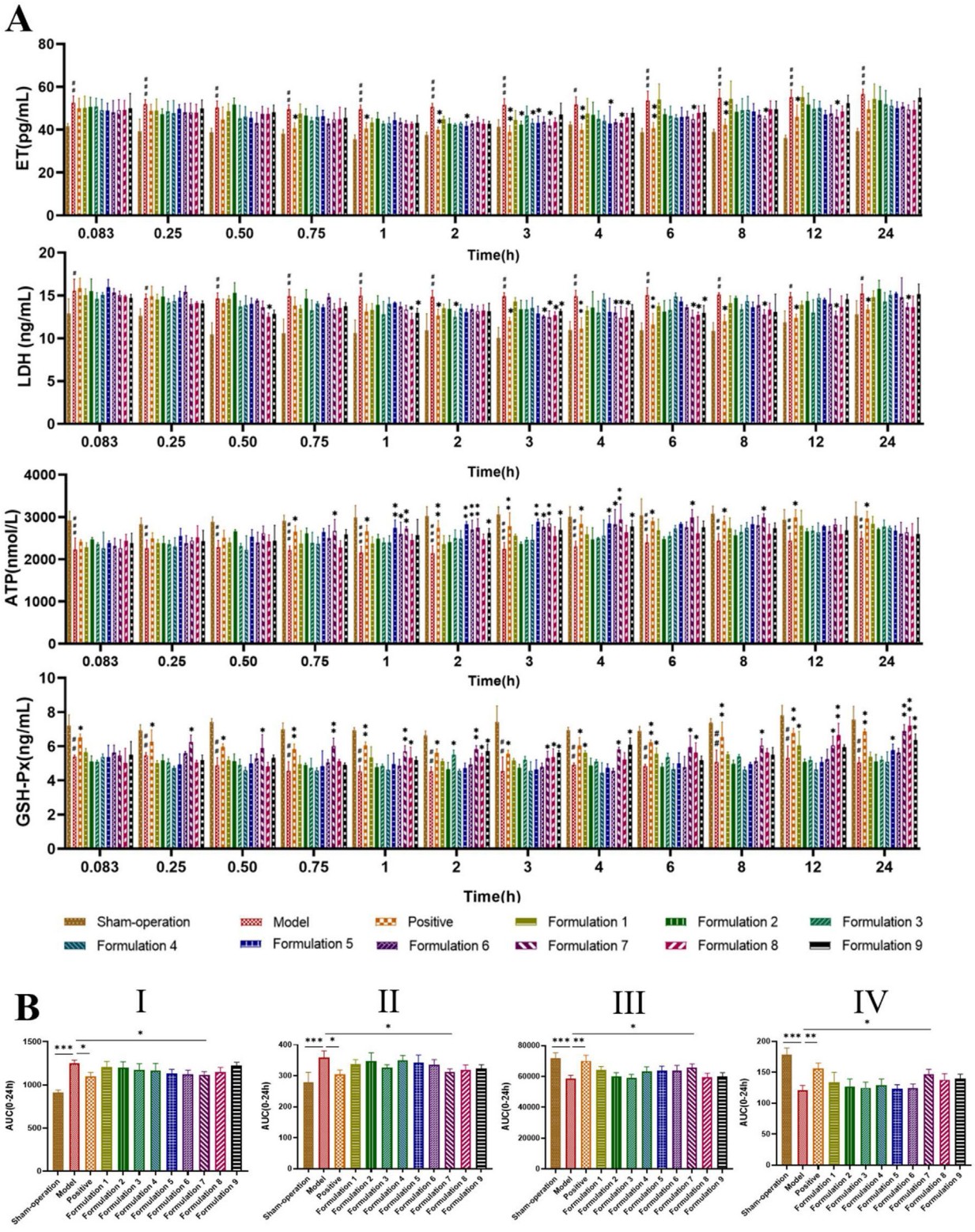

Fig. 3. (A) Effect of different formulations on the ATP, GSH-Px, ET and LDH levels at different time points after intragastric administration; (B) AUCs of LDH (I), ET (II), ATP (III), and GSH-Px (IV) of MCAO/R rats in 24 h after intragastric administration. (Mean ± SD, n = 6). $^{\#}p < 0.05$, $^{\#\#}p < 0.01$ vs sham-operation group; $^{*}p < 0.05$, $^{**}p < 0.01$ vs model group.

Table 5. The optimal PK-PD model equation of analytes. (n = 6).

	ATP	GSH-Px	ET	LDH
CAL	$E = 1619.524*C^{0.434}/(44.832^{0.434}+C^{0.434})$	$E = 1.865*C^{0.402}/36.685^{0.402}+C^{0.402})$	$E = 9.509*C^{0.149}/(46.007^{0.149}+C^{0.149})$	$E = 3.717*C^{4.476}/(0.259^{4.476}+C^{4.476})$
CG	$E = 1626.572*C^{2.071}/(1.229^{2.071}+C^{2.071})$	$E = 0.963*C^{2.777}/(7231.987^{2.777}+C^{2.777})$	$E = 8.593*C^{0.003}/(1.189^{0.003}+C^{0.003})$	$E = 37.817*C^{1.408}/(35.123^{1.408}+C^{1.408})$
FOR	$E = 1172.763*C^{5.719}/(41.849^{5.719}+C^{5.719})$	$E = 16.198*C^{0.836}/(1406.559^{0.836}+C^{0.836})$	$E = 6.561*C^{7.508}/(39.056^{7.508}+C^{7.508})$	$E = 2.054*C^{4.49}/(0.269^{4.49}+C^{4.49})$
ONO	$E = 971.519*C^{4.147}/(11.473^{4.147}+C^{4.147})$	$E = 1.229*C^{4.451}/(10.527^{4.451}+C4.451)$	$E = 6.488*C^{4.269}/(17.069^{4.269}+C^{4.269})$	$E = 3.911*C^{1.002}/(0.168^{1.002}+C^{1.002})$
IG	$E = 1625.257*C^{0.279}/(132.468^{0.279}+C^{0.279})$	$E = 1.893*C^{0.239}/(631.552^{0.239}+C^{0.239})$	$E = 9.54*C^{0.107}/(718.223^{0.107}+C^{0.107})$	$E = 165.094*C^{1.096}/(49.2^{1.096}+C^{1.096})$
DG	$E = 1624.372*C^{0.636}/(27.731^{0.636}+C^{0.636})$	$E = 1.945*C^{0.171}/(26.1^{0.171}+C^{0.171})$	$E = 10.758*C^{0.514}/(27.638^{0.514}+C^{0.514})$	$E = 2.792*C^{1.081}/(0.15^{1.081}+C^{1.081})$
AIV	$E = 1624.965*C^{0.644}/(543.132^{0.644}+C^{0.644})$	$E = 2.025*C^{0.348}/(484.929^{0.348}+C^{0.348})$	$E = 10.949*C^{0.631}/(518.859^{0.631}+C^{0.631})$	$E = 4.72*C^{0.938}/(6.092^{0.938}+C^{0.938})$
AIII	$E = 1624.755*C^{0.888}/(6.715^{0.888}+C^{0.888})$	$E = 1.38*C^{1.195}/(2.390^{1.195}+C^{1.195})$	$E = 12.902*C^{0.853}/(10.474^{0.853}+C^{0.853})$	$E = 11.106*C^{0.569}/(1.021^{0.569}+C^{0.569})$
HYA	$E = 1624.266*C^{0.567}/(3723.387^{0.567}+C^{0.567})$	$E = 2.049*C^{0.528}/(3546.35^{0.528}+C^{0.528})$	$E = 10.039*C^{0.81}/(2959.531^{0.81}+C^{0.81})$	$E = 2.433*C^{2.356}/(10.076^{2.356}+C^{2.356})$
AYB	$E = 1624.297*C^{1.724}/(5.533^{1.724}+C^{1.724})$	$E = 2.206*C^{0.056}/(20794.91^{0.056}+C^{0.056})$	$E = 10.175*C^{0.023}/(25525.77^{0.023}+C^{0.023})$	$E = 62.108*C^{1.118}/(124.929^{1.118}+C^{1.118})$
CAR	$E = 1624.825*C^{0.921}/(134.926^{0.921}+C^{0.921})$	$E = 8.251*C^{0.602}/4412.96^{0.602}+C^{0.602})$	$E = 11.192*C^{0.877}/(152.206^{0.877}+C^{0.877})$	$E = 1.708*C^{2.111}/(61.644^{2.111}+C^{2.111})$

Note: CAL, calycosin; CG, calycosin-7-*O*-β-D-glucoside; FOR, formononetin; ONO, ononin; IG, isomucronulatol 7-*O*-glucoside; DG, 9,10-dimethoxyptercarpan-3-*O*-β-D-glucoside; AIV, astragaloside IV; AIII, astragaloside III; HYA, hydroxysafflor yellow A; AYB, anhydrosafflor yellow B; CAR, carthamin.

7 showed better regulating effect on the disordered biochemical index levels ($p < 0.05$), suggesting that the active fraction combination according to the composition principle of formulation 7 might exerted better anti-CI/RI ability.

3.4. PK and PD correlation analysis

To clarify the correlation between PK and PD, PK-PD modeling was conducted for eleven components in formulation 7 to analyze the links between exposure of eleven components and contents of four efficacy indicators.

The time-concentration-effect curves were fitted by DAS 3.2.6. The larger the adjusted R^2, and smaller the Akaike Information Criterion (AIC) and Bayesian Information Criterion (BIC), the better the model fit. The best-fitting model was selected *via* evaluation of AIC, BIC, and adjusted R^2. The goodness-of-fit information of eleven components was displayed in Suppl. Table 17-20. The optimal PK-PD formulae for analytes were listed in Table 5. There was no one-to-one correspondence between drug concentration and effect after intragastric administration, and maximum effect lagged behind maximum plasma concentration. Moreover, there were anticlockwise hysteretic loops between the concentrations of eleven components and the levels of ATP and GSH-Px, and clockwise hysteretic loops between the concentrations of eleven components and the levels of LDH and ET in the time-concentration-effect curves (Fig. 4). The active compounds in AR-CF were positively or negatively correlated with biochemical factors, indicating the combined synergistic effect of multiple components on MCAO/R rats rather than a single compound extracted from the formulas. PK-PD equation combined with drug concentration and four index effects objectively reflects the regulatory ability of each component to pharmacodynamic indexes.

4. Discussion

TCM provides a large number of effective treatments for various diseases. However, widespread adoption of TCM requires a more comprehensive understanding of the active substances which underpin therapeutic efficacy. For the TCM formulations with multiple active components, the single main component is still taken as the activity index, and the traditional compartment model is used for PK research, which is inconsistent with the overall effect theory embodied in the TCM formulations, nor conducive to the further research on the mechanism and material basis of drug effects [35]. The TQSM

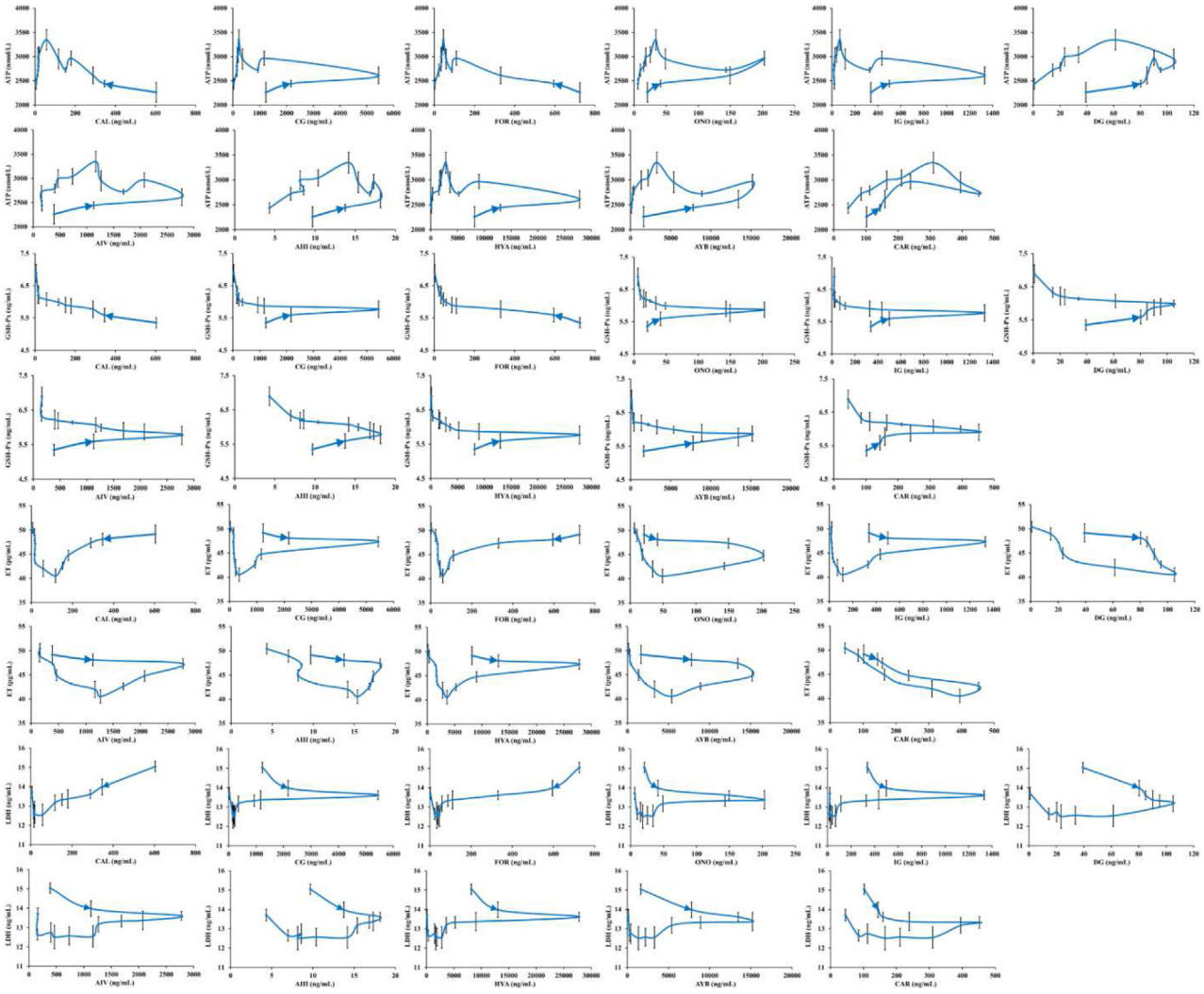

Fig. 4. Time-concentration-effect curves between concentrations of eleven components and ATP, GSH-Px, LDH and ET levels in plasma (Mean ± SD, n = 6). (CAL, calycosin; CG, calycosin-7-O-β-D-glucoside; FOR, formononetin; ONO, ononin; IG, isomucronulatol 7-O-glucoside; DG, 9,10-dimethoxyptercarpan-3-O-β-D-glucoside; AIV, astragaloside IV; AIII, astragaloside III; HYA, hydroxysafflor yellow A; AYB, anhydrosafflor yellow B; CAR, carthamin).

method integrates the pharmacokinetic parameters of single component, and achieves the unification with the total quanta of multiple components [36]. The TQSM method overcomes the limitations of traditional mathematical models and has a wide range of applications, so that more suitable for the overall evaluation of multi-component system of formulation. However, the correlation of obtained pharmacokinetic parameters with pharmacodynamic data is not considered frequently, which leads to difficulties in guiding clinical medication. PK-PD modeling aims to more scientifically and objectively explain the dynamic effects of drugs *in vivo* by correlating the dynamic concentration-time course and effect-time curve, and provides more comprehensive theoretical foundation for the rational usage of drugs.

Effective combination composed of multiple fractions could reflect the characteristics of multi-components and multi-target therapy of TCM or prescription. Effective combination depended on the rational combination of fractions according to appropriate proportion to exert biological activity. It is noteworthy that the effective combination is not a simple combination of multiple active fractions. Each fraction should contribute to the overall efficacy of TCM in different degrees. Based on the results of previous research in our laboratory and literature survey [10,21,22,37], the four important active fractions from AR and CF were selected, using

orthogonal design to combine. The pharmacokinetic parameters of eleven components from different combinations have changed, and their PD *in vivo* have also shown differences. Among the nine formulations, formulation 7, which was composed of 480 mg/kg of flavonoid fraction, 110 mg/kg of saponin fraction, 680 mg/kg of safflower yellow fraction and 480 mg/kg of safflower red fraction, displayed better regulatory effect on the abnormal levels of GSH-Px, ATP, LDH and ET *in vivo*. Moreover, the AUC_T value of eleven components from formulation 7 was the largest among all formulations, and the MRT_T value was similar between formulation 7 and other formulations. The values of AUC_T and MRT_T indirectly reflected the overall situation of components in absorption and elimination *in vivo*. The components in formulation 7 had better absorption and longer retention time *in vivo*. According to the result of variance analysis of TQSM parameters, flavonoid fraction had the greatest contribution to the values of AUC_T and MRT_T, followed by safflower yellow, and finally saponin and safflower red, which was consistent with the combination principle of effective fractions in formulation 7. The saponin and flavonoid were the major active fractions isolated from AR and had been established as two most beneficial fractions. The therapeutic effect of drug will better exerted through the rational combination of active fractions according to the appropriate proportion. Moreover, it is beneficial to better evaluate the anti-CI/RI effect of AR-CF and explore Q-markers by using PK and PD data from formulation 7. The eleven components in formulation 7 were compared holistically for their TQSM poly-pharmacokinetic similarities. The greater TQSM similarity (S_T) of the component, the more important its position in the formulation. Furthermore, by comparing the similarity and AUC of each candidate to TQSM, it was more viable to establish Q-marker screening method [34]. The S_T values of CG, AIV and HYA were 0.9067, 0.9166 and 0.9558. Therefore, CG, AIV and HYA were considered as Q-markers in AR-CF. The screened Q-markers are expected to provide reference indicators for safety and effectiveness of clinical application on a material basis.

GSH-Px is an important *in-vivo* peroxidase, which inhibits production of free radicals, and reduces the damage of organic hydroperoxides to body by removing hydrogen peroxide and lipid hydroperoxides [38]. In the state of ischemia and hypoxia, the systemic stress responses stimulate the increase of ET synthesis and release, and the increase of thrombin in the ischemic area also induces the release of ET, resulting in the abnormal increase of ET *in vivo*. The hypoperfusion induced by vasospasm caused by abnormal increase of ET, is also an important factor leading to brain cell injury [39]. The LDH had been considered as a tissue damage biomarker in many diseases so that its level reflected the degree of tissue damage [40]. ATP is the most direct source of energy in living organisms. When cerebral ischemia occurred, ATP synthesis was blocked and anaerobic metabolism increased *in vivo*. After cerebral ischemia-reperfusion, AR-CF rapidly assisted the generation of ATP and promoted the release of antioxidants, alleviating the further damage of ischemic tissue, and then the contents of ET and LDH in plasma decreased, which indicated that AR-CF played positive role in anti-CI/RI. As the active components were metabolized *in vivo*, the regulation effect of AR-CF on ATP, ET and LDH was gradually weakened, but it still promoted the release of GSH-Px, suggesting that AR-CF exerts anti-CI/RI mainly by inhibiting the generation of free radicals and removing hydrogen peroxide and lipid hydroperoxide.

Through PK and PD modeling, the bio-physiological key characteristics of drugs (potency, efficacy, affinity and specific systemic factors) are discovered, and the extent and duration of drug action under specific pathological conditions are predicted [41]. As a phenomenon reflecting the action state of drugs, hysteresis occasionally occurs in PK-PD modeling. By drawing the time-concentration-effect curve, the hysteresis loop is intuitively observed. It is helpful to describe the hysteresis loop through effect compartment link model [42]. In correlation analysis of PK and PD, the counter-clockwise hysteresis loop is generally regarded as the process of increasing the efficacy over time at given drug concentration. In contrast, the clockwise hysteresis loop implies decrease in effectiveness [43]. It is noteworthy that hysteresis may occur attributable to a consequence of different mechanisms of PK and PD, such as time-dependent protein binding, formation of active metabolites, tolerance, distribution delay, and so on [44]. The correlation was not simple linear, but complex with delayed effect. The plasma drug concentration and efficacy did not reach the peak at the same time, and the peak efficacy obviously lagged behind the plasma drug concentration, indicating that the site of drug action was not in the blood compartment. When cerebral ischemia occurred, the blood−brain barrier was damaged, and active components in AR and CF crossed damaged blood−brain barrier and acted on brain tissue. It takes time for the drugs in the central compartment to be transferred to the effect compartment through the first-order disposition kinetics, so the change of plasma

concentration was not synchronized with the drug effect. Clockwise hysteresis loops were presented in the time-concentration-effect relationships between eleven components and LDH/ET, while the relationship between eleven components and ATP/GSH-Px expressed as anticlockwise hysteresis loops. AR-CF combination up-regulated ATP and GSH-Px levels, and down-regulated LDH and ET levels over time at a given drug concentration. In this experiment, a PK-PD model with an effect compartment was used to analyze the therapeutic material basis and effects of AF-CF combination, which was helpful to better explain the relationship between drug and effects.

5. Conclusions

In summary, the material basis of AR-CF in treatment of CI/RI was explored by the PK-PD analysis of the combination of four active fractions (saponin and flavonoid extracted from AR, and safflower yellow and safflower red extracted from CF). First, a reliable and robust LC-MS/MS approach was developed for the simultaneous determination of eleven components concentrations in rat plasma. The flavonoid fraction was considered to plays an important role for anti-CI/RI in the AR-CF combination through the TQSM method combined with variance analysis of orthogonal experiment. GC, AIV and HYA were identified as Q-markers for AR-CF on CI/RI by TQSM polypharmacokinetics and its similarity approach. Secondly, the contents of biochemical indicators were measured in MCAO/R rats after intragastric administration of nine formulations, respectively. The levels of biochemical indicators in the model group tended to be adjusted to that in sham group after treatment, indicating that AR-CF alleviated CI/RI. Among the nine formulations, formulation 7 had the best regulating effect. Finally, the correlation between candidates and anti-CI/RI efficacy of AR-CF was clarified by PK-PD modeling. This research represents novel study method for the exploration of therapeutic material basis, and provides a more refined compatibility scheme for the TCM prescriptions to exert the best therapeutic effect.

Conflicts of interest

The authors declare no competing financial interests.

Acknowledgements

This research was funded by National Natural Science Foundation of China (No. 82374326), and Zhejiang Provincial Science and Technology Innovation Leading Talent Project of "Ten Thousand Talents Plan" (2019).

Appendix

Flavonoid fraction derived from Astragali Radix (In "2.2 Preparation of herbal active fractions" section)

Astragali Radix powder was imbibed in 54% ethanol with a liquid-to-solid ratio of 18 mL/g. Afterward, heat reflux extraction was performed for 254 min. The extraction solution was filtered, and then concentrated under reduced pressure to obtain the crude extraction solution with the concentration of 0.22 g/mL. The crude extraction solution was purified using a chromatographic column equipped with CAD-40 macroporous resin. The adsorption conditions of purification were as follows: pH value of 6.9, and adsorption flow rate of 1.6 mL/min, while the desorption conditions were as follows: ethanol concentration of 55%, desorption flow rate of 1.5 mL/min and elution volume of 8.5 BV. The eluent was collected and freeze-dried.

Saponin fraction derived from Astragali Radix

Astragali Radix powder was extracted with 50% (v/v) ethanol assisted by microwave for 260 s. The working power was fixed at 695 W, and the ratio of liquid-to-solid was 21.5 mL/g. The extraction solution was evaporated to dryness and redissolved to the concentration of 0.15 g/mL with water, then purified using a chromatographic column equipped with AB-8 macroporous resin. The purification process involved adjusting the pH value of sample to 6.0, loading the sample at an adsorption flow rate of 1.5 mL/min, and eluting with 75% ethanol at a desorption flow rate of 2.0 mL/min and an elution volume of 8 BV. The eluent was collected and freeze-dried.

Safflower red fraction derived from Carthami Flos

An appropriate amount of Carthami Flos powder and 70% acetone solution with a liquid-to-solid ratio of 20 mL/g were placed into a conical flask. The mixture was then extracted using an ultrasonic extractor at 40 °C for 30 min, and the process was repeated twice. The combined filtrate was transferred to a separating funnel and mixed with a supersaturated amount of ammonium sulfate. The upper phase solution was collected and freeze-dried.

Safflower yellow fraction derived from Carthami Flos

Carthami Flos powder was extracted with pure water assisted by ultrasound for 39 min. The working temperature and liquid-to-solid ratio were 55 °C and 16 mL/g. The extraction process was repeated two additional times. The impurities such as polysaccharide and protein in the extraction solution were removed by alcohol precipitation method. The extract was further purified using a chromatographic column equipped with HPD-300 macroporous resin. The concentration of sample was adjusted to 0.06 g/mL. The sample was loaded onto the column at a volume flow rate of 2.5 V/h, followed by washing with deionized water. The column was eluted with 75% ethanol at a volume flow rate of 2.0 V/h. The eluent was collected and freeze-dried.

Suppl. Table 1. Retention time (RT) and MS/MS parameters of the thirteen analytes in MRM analysis.

Compound	RT (min)	Precursor ion (*m/z*)	Product ion (*m/z*)	Declustering Potential/V	Collision Energey/V
Calycosin	15.8	282.9	268.0	−45	−32
Calycosin-7-*O*-*β*-D-glucoside	10.0	447.0	284.9	46	25
Formononetin	24.7	268.9	197.1	96	51
Ononin	12.2	431.0	269.0	41	29
9,10-dimethoxyptercarpan-3-*O*-*β*-D-glucoside	13.7	485.1	323.0	121	31
Isomucronulatol 7-*O*-glucoside	13.8	463.1	286.1	−100	−22
Astragaloside IV	19.7	807.3	627.4	256	65
Astragaloside III	20.5	807.4	334.9	291	73
Carthamin	16.7	909.0	500.9	−100	−38
Hydroxysafflor yellow A	8.1	611.1	491.0	−100	−44
Anhydrosafflor yellow B	10.0	1043.1	449.1	−100	−40
Puerarin	9.0	415.0	295.1	−115	−32
Digoxin	18.6	789.4	651.5	81	21

Suppl. Table 2. Linearity and LLOQ of the eleven analytes in rat plasma.

Components	Regression equation	Linearity range (ng/mL)	Correlation coefficient (R^2)	LLOQ (ng/mL)
Calycosin	$y = 3.40024x+0.00528$	0.5–2000	0.995	0.5
Calycosin-7-*O*-*β*-D-glucoside	$y = 481.91493x+1.25273$	3.5–6000	0.999	3.5
Formononetin	$y = 212.05082x+0.12364$	8.0–2000	0.999	8.0
Ononin	$y = 855.40177x+0.69924$	1.0–2000	0.994	1.0
Isomucronulatol 7-*O*-glucoside	$y = 1.85165x-0.00627$	1.0–2000	0.994	1.0
9,10-dimethoxyptercarpan-3-*O*-*β*-D-glucoside	$y = 1.9209x+0.00385$	10.0–2000	0.998	10.0
Astragaloside IV	$y = 1.10152x+0.00264$	5.0–4000	0.992	5.0
Astragaloside III	$y = 0.35777x+5.26031e^{-4}$	10.0–2000	0.995	10.0
Hydroxysafflor yellow A	$y = 0.05559x+0.00782$	8.0–30000	0.993	8.0
Anhydrosafflor yellow B	$y = 9.27615e^{-4}x+5.68151e^{-4}$	50.0–20000	0.992	50.0
Carthamin	$y = 6.24087e^{-4}x+6.20660e^{-4}$	50.0–10000	0.998	50.0

Suppl. Table 3. Intra- and inter-day precision, accuracy of the eleven analytes in rat plasma. (n = 6)

Components	Spiked concentration (ng/mL)	Intra-day		Inter-day	
		Precision	Accuracy	Precision	Accuracy
		RSD (%)	RE (%)	RSD (%)	RE (%)
Calycosin	0.5	12.41	−2.00	7.31	−1.56
	1.5	4.08	−0.70	4.44	−0.22
	100	11.57	−1.28	9.14	1.16
	2000	3.54	−6.41	5.83	−4.33
Calycosin-7-*O*-*β*-D-glucoside	3.5	3.31	4.40	3.72	2.51
	10.5	8.56	−0.04	9.12	0.86
	100	5.64	8.17	9.40	2.31
	6000	2.63	4.60	5.72	−1.16
Formononetin	8	8.06	−10.83	8.51	−10.60
	24	4.60	−6.82	10.33	2.44
	100	10.56	6.27	9.92	2.08
	2000	11.51	8.45	7.91	3.53
Ononin	1	5.96	−7.67	7.66	−11.89
	3	5.69	−13.67	10.94	−8.48
	100	4.55	12.52	9.58	3.78
	2000	2.29	−6.29	6.73	−1.47
Isomucronulatol 7-*O*-glucoside	1	4.75	−12.33	6.97	−13.33
	3	5.16	9.89	8.32	1.41
	100	10.37	4.95	7.46	7.39
	2000	1.76	−4.22	5.31	−1.12
9,10-dimethoxyptercarpan-3-*O*-*β*-D-glucoside	10	7.26	11.23	7.41	11.42
	30	3.08	10.67	5.36	10.63
	100	5.54	9.00	7.35	10.57
	2000	3.86	12.50	3.62	12.57
Astragaloside IV	5	3.50	−5.30	4.36	−4.53
	15	5.08	−4.00	4.06	−5.99
	100	14.58	3.85	12.26	4.32
	4000	2.05	8.90	4.62	8.66
Astragaloside III	10	2.28	9.90	8.27	10.24
	30	3.08	7.80	4.86	11.17
	100	8.75	3.57	8.75	7.08
	2000	8.65	6.32	8.65	3.08
Hydroxysafflor yellow A	8	5.52	−5.80	4.24	−6.31
	24	6.83	8.58	5.10	9.83
	2000	5.41	−5.65	3.85	−4.12
	30000	2.95	8.18	5.12	12.66
Anhydrosafflor yellow B	50	2.34	6.69	4.58	10.01
	150	3.43	10.69	4.96	13.51
	2000	1.90	8.50	7.43	−0.18
	20000	4.18	13.07	5.88	12.66
Carthamin	50	2.68	−6.84	3.91	−7.08
	150	3.22	−8.18	5.88	−5.85
	2000	12.31	6.23	10.09	9.48
	10000	12.74	11.60	8.55	12.44

Suppl. Table 4. Stability of the eleven analytes in rat plasma. (n = 6)

Components	Spiked concentration (ng/mL)	room temperature for 12 h (RSD%)	4 °C for 24 h (RSD%)	−20 °C for 7 days (RSD%)	After three freezes (at −20 °C)/thaw (at 4 °C) cycle (RSD%)
Calycosin	1.50	7.34	3.38	3.64	8.13
	100	8.93	6.25	6.30	5.73
	2000	9.08	3.69	7.57	6.05
Calycosin-7-*O*-*β*-D-glucoside	10.5	6.40	3.89	7.71	10.83
	100	8.67	5.11	4.04	11.20
	6000	5.28	4.81	3.71	3.56
Formononetin	24	5.04	11.81	4.35	7.69
	100	4.49	6.86	4.80	8.05
	2000	2.89	6.24	6.61	6.90
Ononin	3	4.99	3.48	7.45	4.80
	100	9.65	7.53	8.00	11.50
	2000	6.69	7.48	8.05	7.66
Isomucronulatol 7-*O*-glucoside	3	7.45	8.06	6.97	12.89
	100	7.23	7.94	9.43	9.11
	2000	2.62	7.00	6.53	8.75
9,10-dimethoxyptercarpan-3-*O*-*β*-D-glucoside	30	4.48	5.90	7.84	7.79
	100	10.44	11.04	13.51	9.44
	2000	8.54	14.92	1.95	10.05
Astragaloside IV	15	10.93	3.19	5.37	8.11
	100	12.27	6.07	10.12	5.96
	4000	5.11	8.00	7.93	8.09
Astragaloside III	30	6.78	10.75	10.59	11.24
	100	12.27	8.69	8.41	12.48
	2000	14.91	6.80	5.07	7.11
Hydroxysafflor yellow A	24	9.90	6.30	9.07	7.49
	2000	6.25	5.54	8.51	9.39
	30000	6.23	4.50	6.21	6.33
Anhydrosafflor yellow B	150	2.40	8.98	10.04	9.09
	2000	9.53	7.35	9.81	10.05
	20000	9.69	8.32	8.39	9.18
Carthamin	150	12.64	13.11	13.87	12.11
	2000	7.69	10.81	11.67	11.77
	10000	10.27	13.94	14.33	13.33

Suppl. Table 5. Recovery and matrix effect of the thirteen analytes in rat plasma. (n = 6)

Components	Spiked concentration (ng/mL)	Recovery	Matrix effect
		(Mean ± SD) %	(RSD) %
Calycosin	1.5	86.4 ± 4.3	1.08
	100	85.8 ± 9.2	2.93
	2000	86.5 ± 7.1	2.06
Calycosin-7-*O*-*β*-D-glucoside	10.5	84.8 ± 10.0	3.44
	100	89.8 ± 3.7	2.38
	6000	83.2 ± 11.6	2.61
Formononetin	24	87.7 ± 2.6	5.39
	100	87.6 ± 9.2	2.41
	2000	88.5 ± 11.7	1.95
Ononin	3	84.0 ± 4.4	1.98
	100	90.5 ± 9.8	4.46
	2000	87.3 ± 8.5	3.26
Isomucronulatol 7-*O*-glucoside	3	86.1 ± 10.0	2.21
	100	86.7 ± 5.5	1.17
	2000	85.3 ± 9.2	3.99
9,10-dimethoxyptercarpan-3-*O*-*β*-D-glucoside	30	79.0 ± 1.8	1.93
	100	80.8 ± 4.5	5.32
	2000	78.8 ± 10.2	1.29
Astragaloside IV	15	85.7 ± 12.4	6.38
	100	86.5 ± 6.2	6.22
	4000	85.2 ± 5.4	4.85
Astragaloside III	30	85.5 ± 6.9	3.98
	100	85.2 ± 3.0	7.28
	2000	88.5 ± 8.9	3.15
Hydroxysafflor yellow A	24	86.0 ± 12.6	6.35
	2000	88.5 ± 12.7	7.91
	30000	82.0 ± 11.1	7.97
Anhydrosafflor yellow B	150	85.3 ± 2.0	7.30
	2000	85.6 ± 7.3	7.87
	20000	81.0 ± 9.9	14.68
Carthamin	150	79.5 ± 5.3	10.98
	2000	86.1 ± 8.1	2.13
	10000	77.9 ± 4.1	7.37
Digoxin	1000	87.9 ± 8.3	13.28
Puerarin	100	85.5 ± 9.1	1.96

Suppl. Table 6. The main PK parameters of calycosin in rat plasma after oral administration of different formulations. (Mean ± SD, n = 6)

Parameter	Group								
	formulation 1	formulation 2	formulation 3	formulation 4	formulation 5	formulation 6	formulation 7	formulation 8	formulation 9
$T_{1/2}$(h)	14.41 ± 2.48	10.36 ± 1.66	12.17 ± 1.06	15.91 ± 1.77	10.19 ± 2.01	12.06 ± 1.69	10.84 ± 2.64	8.57 ± 1.01	6.71 ± 0.87
T_{max}(h)	0.14 ± 0.04	0.26 ± 0.07	0.25 ± 0.06	0.17 ± 0.08	0.15 ± 0.05	0.16 ± 0.06	0.11 ± 0.03	0.12 ± 0.01	0.26 ± 0.08
C_{max}(μg/L)	203.21 ± 63.13	115.03 ± 24.11	133.91 ± 21.99	502.32 ± 45.64	839.5 ± 110.21	847.32 ± 97.33	603.74 ± 78.91	856.32 ± 54.52	1434 ± 155.12
$AUC_{(0-t)}$ (μg/L*h)	680.22 ± 55.56	347.43 ± 44.64	466.34 ± 57.51	724.84 ± 65.41	691.47 ± 44.10	716.43 ± 115.12	522.11 ± 77.44	876.96 ± 69.41	1187.09 ± 221.44
$MRT_{(0-t)}$ (h)	6.87 ± 0.64	6.45 ± 0.78	7.22 ± 1.02	7.21 ± 0.99	4.99 ± 0.57	4.89 ± 1.06	5.73 ± 0.79	4.38 ± 0.76	3.38 ± 0.35

Suppl. Table 7. The main PK parameters of calycosin-7-O-β-D-glucoside in rat plasma after oral administration of different formulations. (Mean ± SD, n = 6)

Parameter	Group								
	formulation 1	formulation 2	formulation 3	formulation 4	formulation 5	formulation 6	formulation 7	formulation 8	formulation 9
$T_{1/2}$(h)	21.95 ± 2.36	13.06 ± 1.27	12.26 ± 0.29	11.7 ± 1.55	15.03 ± 2.17	14.41 ± 0.95	15.24 ± 0.74	4.56 ± 0.82	11.09 ± 1.14
T_{max}(h)	0.34 ± 0.09	2.05 ± 0.04	0.32 ± 0.04	0.44 ± 0.06	0.83 ± 0.06	0.53 ± 0.03	0.55 ± 0.06	1.09 ± 0.07	0.59 ± 0.05
C_{max}(μg/L)	537.21 ± 124.12	242.11 ± 48.23	131.84 ± 38.84	468.48 ± 44.14	728.72 ± 63.22	2413.01 ± 359.15	5440.03 ± 486.31	1427.06 ± 157.65	2001.02 ± 312.72
$AUC_{(0-t)}$ (μg/L*h)	833.29 ± 147.35	1313.19 ± 212.66	531.1 ± 96.99	1418.09 ± 87.94	1041.01 ± 102.64	5968.02 ± 634.58	5308.41 ± 589.66	3254.61 ± 478.31	5124.43 ± 229.09
$MRT_{(0-t)}$ (h)	2.95 ± 0.13	6.72 ± 0.54	7.14 ± 0.85	6.03 ± 0.95	2.27 ± 0.18	7.39 ± 0.27	3.04 ± 0.24	3.45 ± 0.67	6.19 ± 1.06

Suppl. Table 8. The main PK parameters of formononetin in rat plasma after oral administration of different formulations. (Mean ± SD, n = 6)

Parameter	Group								
	formulation 1	formulation 2	formulation 3	formulation 4	formulation 5	formulation 6	formulation 7	formulation 8	formulation 9
$T_{1/2}$(h)	6.71 ± 1.02	6.18 ± 1.13	8.63 ± 0.64	5.04 ± 0.76	7.86 ± 0.89	5.18 ± 0.62	8.23 ± 0.92	18.54 ± 2.15	10.45 ± 1.47
T_{max}(h)	0.12 ± 0.05	0.15 ± 0.01	0.25 ± 0.05	0.11 ± 0.04	0.10 ± 0.01	0.09 ± 0.02	0.11 ± 0.04	0.14 ± 0.07	0.12 ± 0.03
C_{max}(μg/L)	193.32 ± 19.55	119.78 ± 21.22	117.12 ± 18.46	272.31 ± 32.12	344.56 ± 46.78	228.91 ± 56.11	725.69 ± 121.66	717.71 ± 98.44	667 ± 102.77
$AUC_{(0-t)}$ (μg/L*h)	249.04 ± 63.36	236.47 ± 74.26	287.07 ± 52.25	302.67 ± 69.65	295.35 ± 71.47	229.51 ± 74.17	289.28 ± 23.23	528.05 ± 98.31	763.16 ± 88.68
$MRT_{(0-t)}$ (h)	3.17 ± 0.57	8.52 ± 0.98	4.9 ± 0.15	2.85 ± 0.35	2.21 ± 0.54	6.03 ± 0.75	2.01 ± 0.14	3.71 ± 0.21	6.04 ± 1.08

Suppl. Table 9. The main PK parameters of ononin in rat plasma after oral administration of different formulations. (Mean ± SD, n = 6)

Parameter	Group								
	formulation 1	formulation 2	formulation 3	formulation 4	formulation 5	formulation 6	formulation 7	formulation 8	formulation 9
$T_{1/2}$(h)	6.16 ± 0.84	15.14 ± 1.05	17.02 ± 1.07	12.72 ± 0.68	12.67 ± 0.77	15.82 ± 1.28	17.34 ± 1.04	14.45 ± 1.13	10.24 ± 0.28
T_{max}(h)	0.86 ± 0.08	0.75 ± 0.04	0.58 ± 0.05	0.51 ± 0.06	0.77 ± 0.07	0.55 ± 0.05	0.71 ± 0.05	1.04 ± 0.07	0.61 ± 0.08
C_{max}(μg/L)	164.61 ± 35.54	178.82 ± 32.51	187.52 ± 25.15	439.7 ± 25.65	171.42 ± 23.12	1101.56 ± 162.13	242.98 ± 26.15	368.6 ± 36.88	508.84 ± 46.56
$AUC_{(0-t)}$ (μg/L*h)	319.65 ± 45.64	1133.75 ± 96.64	367.27 ± 42.16	3009.78 ± 221.06	736.27 ± 54.45	1156.21 ± 166.64	550.05 ± 34.16	897.42 ± 68.91	1865.38 ± 264.16
$MRT_{(0-t)}$ (h)	4.28 ± 0.45	8.72 ± 0.68	6.84 ± 0.66	9.54 ± 0.72	7.89 ± 1.07	3.94 ± 0.21	6.36 ± 0.74	5.03 ± 0.46	8.02 ± 0.87

Suppl. Table 10. The main PK parameters of isomucronulatol 7-O-glucoside in rat plasma after oral administration of different formulations. (Mean ± SD, n = 6)

Parameter	Group								
	formulation 1	formulation 2	formulation 3	formulation 4	formulation 5	formulation 6	formulation 7	formulation 8	formulation 9
$T_{1/2}$(h)	12.21 ± 1.54	10.79 ± 2.52	11.36 ± 3.54	8.59 ± 2.12	16.83 ± 2.34	18.36 ± 3.87	10.41 ± 1.59	14.3 ± 0.98	9.38 ± 1.07
T_{max}(h)	0.84 ± 0.12	0.79 ± 0.24	0.65 ± 0.16	0.71 ± 0.09	0.69 ± 0.56	0.59 ± 0.19	0.57 ± 0.11	1.06 ± 0.41	0.58 ± 0.08
C_{max}(μg/L)	266.61 ± 12.25	257.25 ± 15.97	348.01 ± 42.12	751.24 ± 24.13	897.56 ± 56.89	843.52 ± 123.87	1331.45 ± 251.22	1164.47 ± 245.23	1206.5 ± 274.25
$AUC_{(0-t)}$ (μg/L*h)	499.42 ± 96.15	434.36 ± 145.65	371.28 ± 65.42	1661.32 ± 351.25	1103.95 ± 128.98	1463.29 ± 426.56	1385.05 ± 200.21	1611.12 ± 298.64	1502.11 ± 318.29
$MRT_{(0-t)}$ (h)	5.56 ± 0.45	6.17 ± 25	6.41 ± 0.64	3.81 ± 0.12	1.83 ± 0.46	3.79 ± 0.31	5.51 ± 1.02	5.16 ± 0.23	4.79 ± 0.64

Suppl. Table 11. The main PK parameters of 9,10-dimethoxyptercarpan-3-O-β-D-glucoside in rat plasma after oral administration of different formulations. (Mean ± SD, n = 6)

Parameter	Group								
	formulation 1	formulation 2	formulation 3	formulation 4	formulation 5	formulation 6	formulation 7	formulation 8	formulation 9
$T_{1/2}$(h)	6.98 ± 0.74	12.63 ± 0.69	14.55 ± 0.92	6.87 ± 0.58	9.31 ± 0.67	6.77 ± 0.77	3.53 ± 0.35	4.73 ± 0.44	12.25 ± 1.05
T_{max}(h)	0.79 ± 0.11	0.58 ± 0.05	0.55 ± 0.04	0.51 ± 0.06	0.78 ± 0.07	0.64 ± 0.06	2.01 ± 0.14	1.11 ± 0.25	0.64 ± 0.07
C_{max}(μg/L)	148.56 ± 22.01	139.49 ± 19.99	612 ± 44.32	268.1 ± 41.32	182.2 ± 20.01	348.65 ± 45.12	104.5 ± 19.16	234.12 ± 41.02	564.7 ± 66.32
$AUC_{(0-t)}$ (μg/L*h)	377.54 ± 31.10	608.78 ± 77.64	3073.78 ± 226.45	2072.65 ± 251.64	416.19 ± 36.49	123.05 ± 24.11	567.56 ± 69.45	546.74 ± 62.15	1750.18 ± 196.64
$MRT_{(0-t)}$ (h)	4.54 ± 0.55	7.93 ± 0.46	9.29 ± 0.37	8.49 ± 0.49	4.48 ± 0.61	6.99 ± 1.05	5.65 ± 0.96	3.51 ± 0.43	7.42 ± 0.85

Suppl. Table 12. The main PK parameters of astragaloside IV in rat plasma after oral administration of different formulations. (Mean ± SD, n = 6)

Parameter	Group								
	formulation 1	formulation 2	formulation 3	formulation 4	formulation 5	formulation 6	formulation 7	formulation 8	formulation 9
$T_{1/2}$(h)	12.16 ± 1.08	12.05 ± 1.13	8.25 ± 0.85	18.35 ± 0.96	10.87 ± 1.05	10.92 ± 1.21	12.34 ± 0.99	10.75 ± 0.46	7.82 ± 1.04
T_{max}(h)	0.79 ± 0.09	0.70 ± 0.10	0.81 ± 0.06	3.04 ± 0.24	0.95 ± 0.04	1.06 ± 0.11	0.64 ± 0.04	0.94 ± 0.13	0.68 ± 0.02
C_{max}(μg/L)	311.91 ± 23.01	217.12 ± 41.51	625.65 ± 66.48	196.7 ± 11.21	211.43 ± 19.96	1179.06 ± 223.25	2776.87 ± 336.44	836.11 ± 114.25	1037.03 ± 156.36
$AUC_{(0-t)}$ (μg/L*h)	1035.18 ± 144.44	729.53 ± 195.78	1562.07 ± 280.09	1547.56 ± 115.17	703.82 ± 124.45	7965.3 ± 634.17	10158.82 ± 1005.65	4010.21 ± 685.21	4753.63 ± 578.33
$MRT_{(0-t)}$ (h)	4.98 ± 0.68	4.97 ± 0.99	4.42 ± 0.86	8.11 ± 1.08	4.75 ± 0.11	7.9 ± 0.68	6.42 ± 0.75	6.35 ± 0.94	5.91 ± 0.77

Suppl. Table 13. The main PK parameters of astragaloside III in rat plasma after oral administration of different formulations. (Mean ± SD, n = 6)

Parameter	Group								
	formulation 1	formulation 2	formulation 3	formulation 4	formulation 5	formulation 6	formulation 7	formulation 8	formulation 9
$T_{1/2}$(h)	13.25 ± 1.49	15.77 ± 2.06	13.91 ± 2.45	15.47 ± 1.48	15.77 ± 1.88	13.17 ± 1.08	11.72 ± 1.44	13.48 ± 1.29	13.82 ± 1.78
T_{max}(h)	0.79 ± 0.06	0.85 ± 0.05	0.64 ± 0.03	0.55 ± 0.07	0.75 ± 0.18	0.57 ± 0.04	0.59 ± 0.05	0.78 ± 0.07	0.54 ± 0.02
C_{max}(μg/L)	71.63 ± 3.54	49.97 ± 10.25	110.29 ± 21.22	20.95 ± 5.64	48.83 ± 5.97	53.1 ± 12.64	36.32 ± 9.81	49.37 ± 10.64	123.21 ± 18.61
$AUC_{(0-t)}$ (μg/L*h)	298.97 ± 29.64	257.15 ± 35.26	394.06 ± 37.87	193.91 ± 39.44	260.61 ± 28.89	236.89 ± 25.47	326.461 ± 41.52	314.77 ± 174.16	388.47 ± 169.63
$MRT_{(0-t)}$ (h)	9.11 ± 1.09	8.26 ± 1.47	7.55 ± 0.87	9.27 ± 0.44	8.15 ± 0.68	7.81 ± 0.97	7.99 ± 1.08	8.27 ± 1.44	7.29 ± 1.99

Suppl. Table 14. The main PK parameters of hydroxysafflor yellow A in rat plasma after oral administration of different formulations. (Mean ± SD, n = 6)

Parameter	Group								
	formulation 1	formulation 2	formulation 3	formulation 4	formulation 5	formulation 6	formulation 7	formulation 8	formulation 9
$T_{1/2}$(h)	10.91 ± 1.06	15.52 ± 1.17	7.97 ± 0.96	17.33 ± 0.48	11.01 ± 1.06	9.51 ± 1.27	18.95 ± 1.96	11.84 ± 0.96	9.51 ± 0.88
T_{max}(h)	1.04 ± 0.23	0.79 ± 0.19	0.35 ± 0.09	1.11 ± 0.06	0.78 ± 0.08	2.11 ± 0.25	0.58 ± 0.04	0.77 ± 0.05	0.66 ± 0.04
C_{max}(μg/L)	8040.12 ± 552.06	8302.05 ± 414.14	4435.22 ± 298.69	2296.31 ± 252.45	20590.01 ± 1548.94	4385.04 ± 354.21	27770.06 ± 1974.44	11970.25 ± 1064.22	15650.2 ± 1232.08
$AUC_{(0-t)}$ (μg/L*h)	22514.55 ± 1421.49	9252.02 ± 212.21	16325.79 ± 1456.28	7390.05 ± 365.54	36045.26 ± 1946.61	21639.42 ± 1783.26	40825.12 ± 2001.4	36872.11 ± 1889.51	36370.11 ± 1639.77
$MRT_{(0-t)}$ (h)	7.54 ± 1.23	6.47 ± 0.25	8.11 ± 0.66	8.56 ± 0.76	3.42 ± 0.34	5.85 ± 0.46	5.89 ± 0.64	6.11 ± 0.74	4.71 ± 0.69

Suppl. Table 15. The main PK parameters of anhydrosafflor yellow B in rat plasma after oral administration of different formulations. (Mean ± SD, n = 6)

Parameter	Group								
	formulation 1	formulation 2	formulation 3	formulation 4	formulation 5	formulation 6	formulation 7	formulation 8	formulation 9
$T_{1/2}$(h)	17.84 ± 1.22	10.65 ± 0.95	8.86 ± 0.44	11.04 ± 1.06	20.65 ± 2.58	10.17 ± 1.05	11.73 ± 1.21	5.05 ± 0.25	11.21 ± 0.64
T_{max}(h)	1.21 ± 0.22	0.79 ± 0.11	0.58 ± 0.05	0.48 ± 0.02	0.39 ± 0.04	0.64 ± 0.07	0.71 ± 0.04	0.76 ± 0.09	1.05 ± 0.03
C_{max}(μg/L)	4232.45 ± 264.54	2913.04 ± 623.21	7272.05 ± 456.21	2929.05 ± 194.26	4053.02 ± 189.52	11990 ± 678.88	16180.25 ± 1125.54	4208.05 ± 214.12	7543.14 ± 335.77
$AUC_{(0-t)}$ (μg/L*h)	13037.64 ± 1101.56	8535.66 ± 636.58	32295.34 ± 1985.89	9439.2 ± 457.55	8422.52 ± 458.52	19378.86 ± 1487.64	23141.43 ± 864.19	8322.75 ± 565.22	10533.37 ± 697.44
$MRT_{(0-t)}$ (h)	7.08 ± 0.64	7.07 ± 0.78	5.25 ± 0.22	7.19 ± 0.56	4.86 ± 0.47	7.77 ± 0.98	5.46 ± 0.15	5.04 ± 0.54	4.01 ± 1.59

Suppl. Table 16. The main PK parameters of carthamin in rat plasma after oral administration of different formulations. (Mean ± SD, n = 6)

Parameter	Group								
	formulation 1	formulation 2	formulation 3	formulation 4	formulation 5	formulation 6	formulation 7	formulation 8	formulation 9
$T_{1/2}$(h)	5.96 ± 0.78	7.03 ± 1.05	5.78 ± 0.96	6.4 ± 0.46	4.96 ± 0.62	6.39 ± 0.74	6.28 ± 0.74	6.14 ± 0.66	6.19 ± 0.61
T_{max}(h)	1.12 ± 0.11	1.21 ± 0.13	1.07 ± 0.48	0.79 ± 0.22	1.11 ± 0.05	0.58 ± 0.06	1.07 ± 0.09	0.79 ± 0.08	1.07 ± 0.07
C_{max}(μg/L)	1677.45 ± 264.16	465.15 ± 65.21	751.15 ± 45.56	9518 ± 355.05	732.1 ± 74.36	3285 ± 325.14	452.12 ± 36.18	501.12 ± 41.08	298.4 ± 45.25
$AUC_{(0-t)}$ (μg/L*h)	3145.31 ± 226.64	2692.89 ± 198.54	3612.89 ± 332.45	20100.7 ± 987.98	2391.29 ± 364.21	6298.82 ± 478.77	3996.49 ± 269.48	2510.01 ± 199.88	2761.95 ± 206.94
$MRT_{(0-t)}$ (h)	3.75 ± 0.64	6.76 ± 0.98	5.11 ± 1.03	4.08 ± 0.66	5.06 ± 0.78	4.91 ± 0.92	6.01 ± 0.86	6.55 ± 0.69	6.21 ± 1.04

Suppl. Table 17. The best compartmental model parameters attained by fitting the △LDH and the concentrations of 11 components.

	CAL	CG	FOR	ONO	IG	DG	AIV	AIII	HYA	AYB	AYB
AIC	25.304	21.743	9.858	69.189	6.261	20.336	9.904	3.819	18.577	219.261	14.08
BIC	28.213	24.652	12.767	72.098	9.17	23.245	13.783	6.728	21.487	222.17	17.959
R^2	0.94	0.985	0.937	0.936	0.949	0.915	0.914	0.923	0.936	0.958	0.957

Note: AIC, Akaike Information Criterion; BIC, Bayesian Information Criterion; CAL, calycosin; CG, calycosin-7-O-β-D-glucoside; FOR, formononetin; ONO, ononin; IG, isomucronulatol 7-O-glucoside; DG, 9,10-dimethoxyptercarpan-3-O-β-D-glucoside; AIV, astragaloside IV; AIII, astragaloside III; HYA, hydroxysafflor yellow A; AYB, anhydrosafflor yellow B; CAR, carthamin.

Suppl. Table 18. The best compartmental model parameters attained by fitting the △ATP and the concentrations of 11 components.

	CAL	CG	FOR	ONO	IG	DG	AIV	AIII	HYA	AYB	AYB
AIC	39.483	22.06	9.858	15.316	6.261	21.037	9.904	4.493	18.57	219.261	14.08
BIC	43.362	25.939	12.767	19.195	9.17	24.916	13.783	8.372	22.449	222.17	17.959
R^2	0.981	0.930	0.937	0.919	0.949	0.917	0.914	0.904	0.959	0.958	0.957

Suppl. Table 19. The best compartmental model parameters attained by fitting the △GSH-Px and the concentrations of 11 components.

	CAL	CG	FOR	ONO	IG	DG	AIV	AIII	HYA	AYB	AYB
AIC	39.483	10.31	63.279	15.316	13.394	21.037	9.904	3.819	18.57	219.261	14.08
BIC	43.362	14.19	66.188	19.195	17.274	24.916	13.783	6.728	22.449	222.17	17.959
R^2	0.981	0.968	0.988	0.919	0.946	0.917	0.914	0.923	0.959	0.958	0.957

Suppl. Table 20. The best compartmental model parameters attained by fitting the △ET and the concentrations of 11 components.

	CAL	CG	FOR	ONO	IG	DG	AIV	AIII	HYA	AYB	AYB
AIC	39.483	10.31	9.858	15.948	6.261	21.037	9.904	4.493	125.906	219.261	14.08
BIC	43.362	14.19	12.767	19.827	9.17	24.916	13.783	8.372	129.785	222.17	17.959
R^2	0.981	0.968	0.937	0.937	0.949	0.917	0.914	0.904	0.994	0.958	0.957

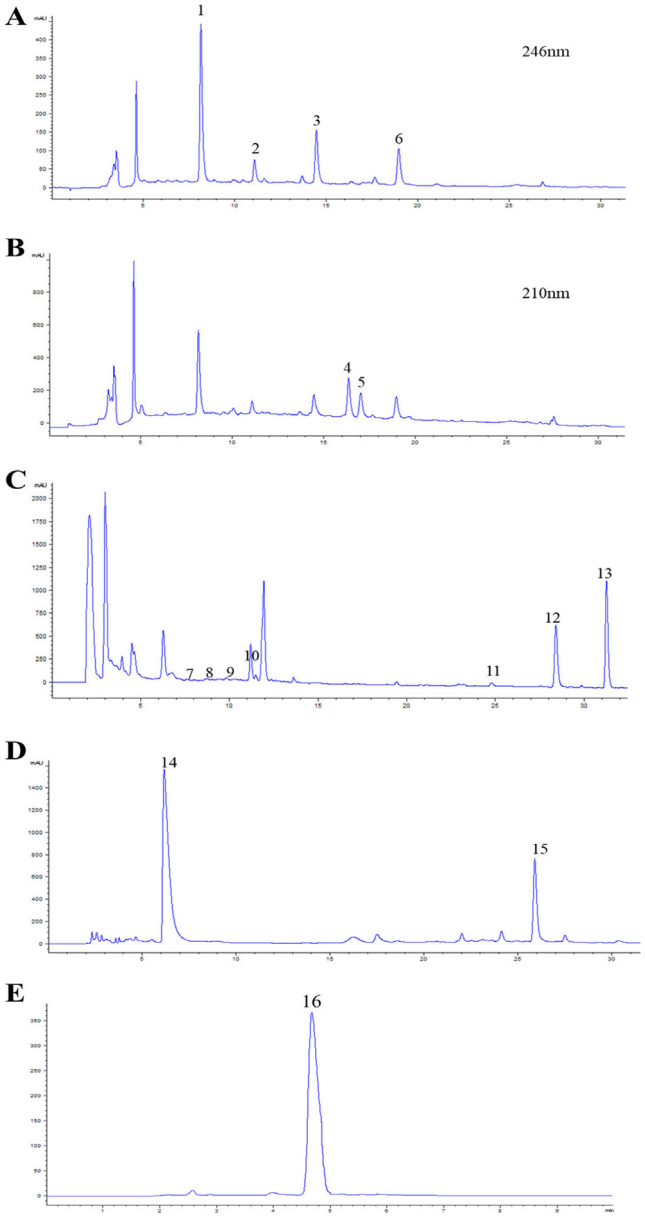

Suppl. Fig. 1. HPLC chromatogram of the flavonoid (A and B) and saponin (C) from Astragali Radix and the safflower yellow (D) and safflower red (E) from Carthami Flos. 1. calycosin-7-O-β-D-glucoside; 2. ononin; 3. 9,10-dimethoxyptercarpan-3-O-β-D-glucoside; 4. isomucronulatol 7-O-glucoside; 5. calycosin; 6. formononetin; 7. astragaloside V; 8. astragaloside IV; 9. astragaloside III; 10. astragaloside II; 11. astragaloside I; 12. isoastragaloside I; 13. isoastragaloside II; 14. hydroxysafflor yellow A; 15. anhydrosafflor yellow B; 16. carthamin. (The components 7, 10, 11, 12, and 13 were undetected in rat plasma within 24 h of administration, so these five components were not included in the detection index of PK).

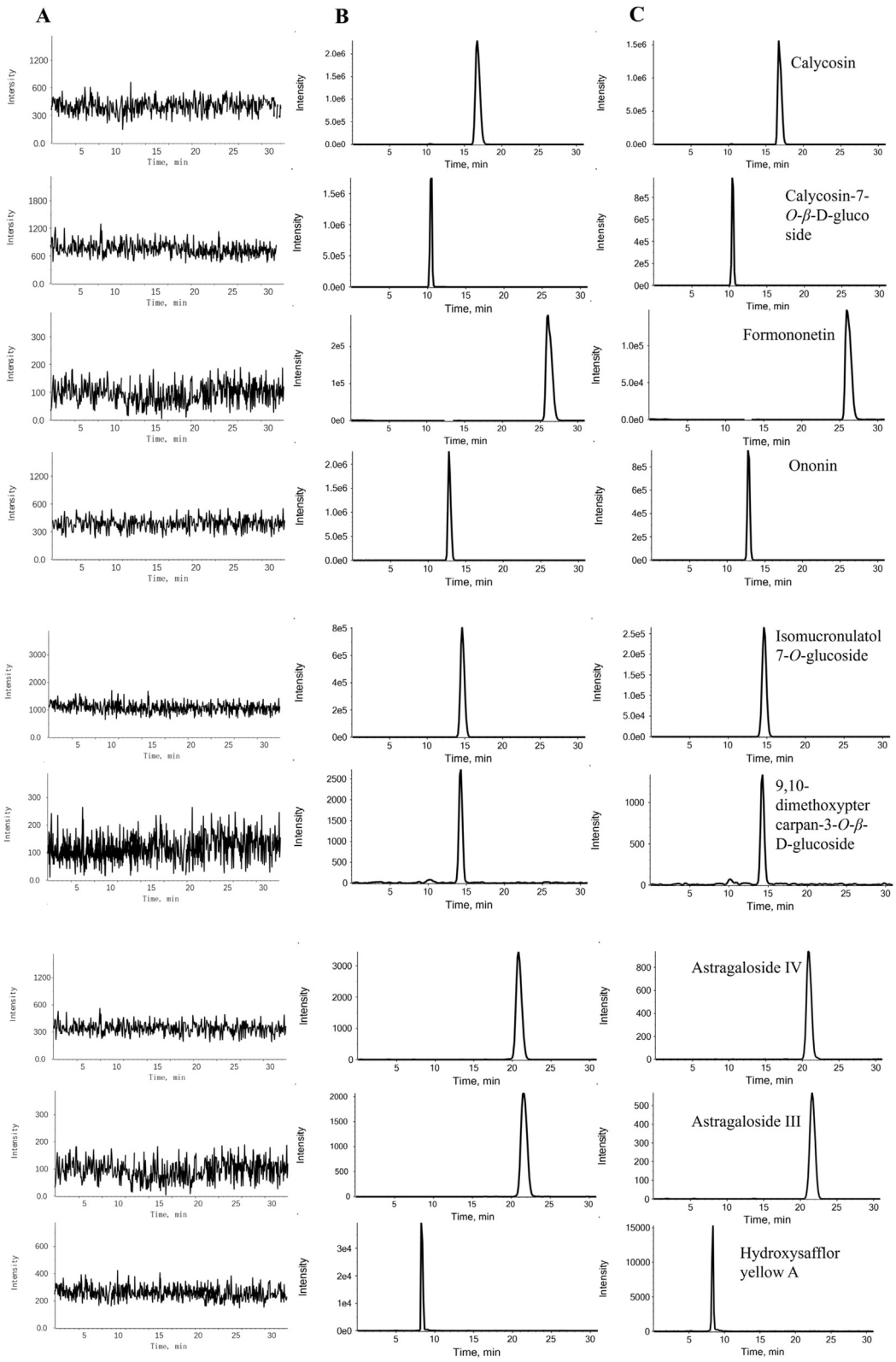

Suppl. Fig. 2. (Continued).

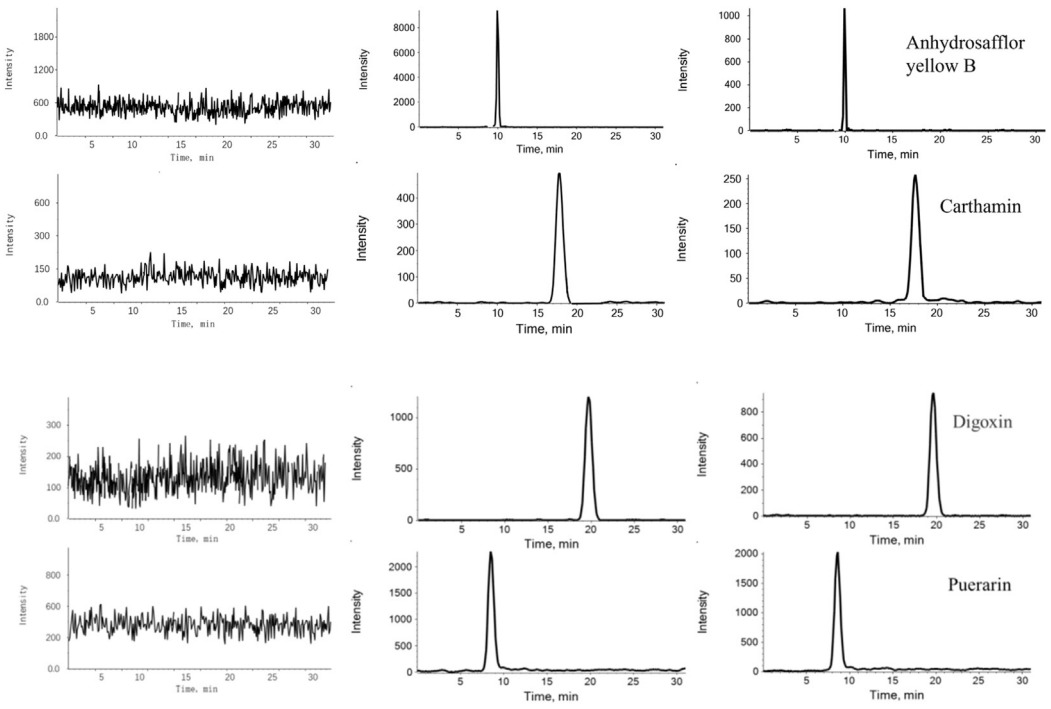

Suppl. Fig. 2. Typical MRM chromatograms of (A) blank plasma; (B) blank plasma spiked with analytes and ISs; (C) 0.5 h analytes and ISs of plasma after oral administration of AR-CF.

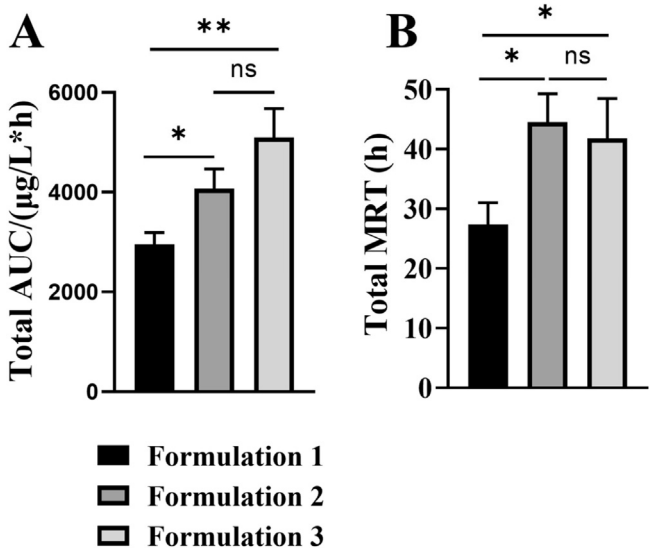

Suppl. Fig. 3. The AUC (A) and MRT (B) of flavonoid compounds (as a whole) from Astragali Radix in formulation 1, 2, and 3.

References

[1] Zhang J, Liu W, Bi M, Xu J, Yang H, Zhang Y. Noble gases therapy in cardiocerebrovascular diseases: the novel stars? Front Cardiovasc Med 2022;9:802783.
[2] Sun MS, Jin H, Sun X, Huang S, Zhang FL, Guo ZN, et al. Free radical damage in ischemia-reperfusion injury: an obstacle in acute ischemic stroke after revascularization therapy. Oxid Med Cell Longev 2018;2018:3804979.
[3] Hong L, Chen W, He L, Tan H, Peng D, Zhao G, et al. Effect of Naoluoxintong on the NogoA/RhoA/ROCK pathway by down-regulating DNA methylation in MCAO rats. J Ethnopharmacol 2021;281:114559.
[4] Paul S, Candelario-Jalil E. Emerging neuroprotective strategies for the treatment of ischemic stroke: an overview of clinical and preclinical studies. Exp Neurol 2021;335:113518.
[5] Sekerdag E, Solaroglu I, Gursoy-Ozdemir Y. Cell death mechanisms in stroke and novel molecular and cellular

treatment options. Curr Neuropharmacol 2018;16: 1396−415.
[6] Luo Y, Wang CZ, Hesse-Fong J, Lin JG, Yuan CS. Application of Chinese medicine in acute and critical medical conditions. Am J Chin Med 2019;47:1223−35.
[7] Liao H, Banbury L. Different proportions of Huangqi (Radix Astragali mongolici) and Honghua (Flos Carthami) injection on alpha-glucosidase and alpha-amylase activities. Evid Based Compl Alternat Med 2015;2015:785193.
[8] Chen X, Chen H, He Y, Fu S, Liu H, Wang Q, et al. Proteomics-guided study on Buyang Huanwu decoction for its neuroprotective and neurogenic mechanisms for transient ischemic stroke: involvements of EGFR/PI3K/Akt/Bad/14-3-3 and Jak2/stat3/cyclin D1 signaling cascades. Mol Neurobiol 2020;57:4305−21.
[9] Cao J, Chen Z, Zhu Y, Li Y, Guo C, Gao K, et al. Huangqi-Honghua combination and its main components ameliorate cerebral infarction with Qi deficiency and blood stasis syndrome by antioxidant action in rats. J Ethnopharmacol 2014; 155:1053−60.
[10] Wang Y, Liu X, Hu T, Li X, Chen Y, Xiao G, et al. Astragalus saponins improves stroke by promoting the proliferation of neural stem cells through phosphorylation of Akt. J Ethnopharmacol 2021;277:114224.
[11] Zou Y, Li S, Chen T, Li Z, Gao X, Wang Z. Astragaloside IV ameliorates peripheral immunosuppression induced by cerebral ischemia through inhibiting HPA axis. Int Immunopharm 2022;105:108569.
[12] Guo H, Zhu L, Tang P, Chen D, Li Y, Li J, et al. Carthamin yellow improves cerebral ischemiareperfusion injury by attenuating inflammation and ferroptosis in rats. Int J Mol Med 2021;47:52.
[13] Sheng Z, Jiang Y, Liu J, Yang B. UHPLC-MS/MS analysis on flavonoids composition in *Astragalus membranaceus* and their antioxidant activity. Antioxidants 2021;10:1852.
[14] Fu J, Wang Z, Huang L, Zheng S, Wang D, Chen S, et al. Review of the botanical characteristics, phytochemistry, and pharmacology of Astragalus membranaceus (Huangqi). Phytother Res 2014;28:1275−83.
[15] Zhang LL, Tian K, Tang ZH, Chen XJ, Bian ZX, Wang YT, et al. Phytochemistry and pharmacology of Carthamus tinctorius L. Am J Chin Med 2016;44:197−226.
[16] Gu S, Cao B, Sun R, Tang Y, Paletta JL, Wu X, et al. A metabolomic and pharmacokinetic study on the mechanism underlying the lipid-lowering effect of orally administered berberine. Mol Biosyst 2015;11:463−74.
[17] Milligan PA, Brown MJ, Marchant B, Martin SW, van der Graaf PH, Benson N, et al. Model-based drug development: a rational approach to efficiently accelerate drug development. Clin Pharmacol Ther 2013;93:502−14.
[18] Deng R, Wang W, Wu H, Zhang Y, Wang W, Dai L, et al. A microdialysis in adjuvant arthritic rats for Pharmacokinetics(-)Pharmacodynamics modeling study of geniposide with determination of drug concentration and efficacy levels in dialysate. Molecules 2018;23.
[19] Kong X, Wang F, Niu Y, Wu X, Pan Y. A comparative study on the effect of promoting the osteogenic function of osteoblasts using isoflavones from Radix Astragalus. Phytother Res 2018;32:115−24.
[20] Ao H, Feng W, Peng C. Hydroxysafflor yellow A: a promising therapeutic agent for a broad spectrum of diseases. Evid Based Compl Alternat Med 2018;2018:8259280.
[21] Hiramatsu M, Takahashi T, Komatsu M, Kido T, Kasahara Y. Antioxidant and neuroprotective activities of Mogami-benibana (safflower, Carthamus tinctorius Linne). Neurochem Res 2009;34:795−805.
[22] Chen G, Li C, Zhang L, Yang J, Meng H, Wan H, et al. Hydroxysafflor yellow A and anhydrosafflor yellow B alleviate ferroptosis and parthanatos in PC12 cells injured by OGD/R. Free Radic Biol Med 2022;179:1−10.
[23] Sun Y, He Y, Zhang R, Huang J, Gu M. Optimization of ultrasonic extraction conditions of safflower yellower from Carthamus tinctorius by response surface methodology. J Chin Med Mater 2013;36:2018−22.
[24] Liu Q, Chen X, Yu P, Jin L, He J. Extraction of carthamine from Flos Carthami by combining ultrasonic extraction and aqueous two-phase system separation technique. Chin Pharmaceut J 2011;46:1482−5.
[25] Xu S, Wan H, Zhao X, Zhang Y, Yang J, Jin W, et al. Optimization of extraction and purification processes of six flavonoid components from Radix Astragali using BP neural network combined with particle swarm optimization and genetic algorithm. Ind Crop Prod 2022;178:114556.
[26] Du Y, Huang P, Jin W, Li C, Yang J, Wan H, et al. Optimization of extraction or purification process of multiple components from natural products: entropy weight method combined with plackett-Burman design and central composite design. Molecules 2021;26:5572.
[27] Meesters RJW, Voswinkel S. Bioanalytical method development and validation: from the USFDA 2001 to the USFDA 2018 guidance for industry. J Appl Bioanal 2018;4:67−73.
[28] Shi X, Yu W, Liu L, Liu W, Zhang X, Yang T, et al. Panax notoginseng saponins administration modulates pro-/anti-inflammatory factor expression and improves neurologic outcome following permanent MCAO in rats. Metab Brain Dis 2017;32:221−33.
[29] Carlson AP, Hanggi D, Macdonald RL, Shuttleworth CW. Nimodipine reappraised: an old drug with a future. Curr Neuropharmacol 2020;18:65−82.
[30] Wang Y, He S, Liu X, Li Z, Zhu L, Xiao G, et al. Galectin-3 mediated inflammatory response contributes to neurological recovery by QiShenYiQi in subacute stroke model. Front Pharmacol 2021;12:588587.
[31] Wang Y, Wu H, Han Z, Sheng H, Wu Y, Wang Y, et al. Guhong injection promotes post-stroke functional recovery via attenuating cortical inflammation and apoptosis in subacute stage of ischemic stroke. Phytomedicine 2022;99: 154034.
[32] Committee NP. Pharmacopoeia of people's Republic of China. Beijing. 2020.
[33] Ying Y, Wan H, Zhao X, Yu L, He Y, Jin W. Pharmacokinetic-pharmacodynamic modeling of the antioxidant activity of Quzhou fructus aurantii decoction in a rat model of hyperlipidemia. Biomed Pharmacother 2020;131:110646.
[34] Zhang YT, Xiao MF, Liao Q, Liu WL, Deng KW, Zhou YQ, et al. Application of TQSM polypharmacokinetics and its similarity approach to ascertain Q-marker by analyses of transitivity in vivo of five candidates in Buyanghuanwu injection. Phytomedicine 2018;45:18−25.
[35] Li Q, Yang Y, Zhou T, Wang R, Li N, Zheng M, et al. A Compositive Strategy to Study the Pharmacokinetics of TCMs: taking Coptidis Rhizoma, and Coptidis Rhizoma-Glycyrrhizae Radix et Rhizoma as Examples. Molecules 2018; 23.
[36] Yan YL, Dai XY. Total quantity statistical moment analysis on pharmacokinetics of rhein and chrysophanol after oral administration of Quyu Qingre granules in normal and acute blood stasis rabbits. China J Chin Mater Med 2014;39: 520−5.
[37] Liu Q, Zhang L, Shan Q, Ding Y, Zhang Z, Zhu M, et al. Total flavonoids from Astragalus alleviate endothelial dysfunction by activating the Akt/eNOS pathway. J Int Med Res 2018;46: 2096−103.
[38] Wang T, Lin S, Li H, Liu R, Liu Z, Xu H, et al. A stepwise integrated multi-system to screen quality markers of Chinese classic prescription Qingzao Jiufei decoction on the treatment of acute lung injury by combining 'network pharmacology-metabolomics-PK/PD modeling'. Phytomedicine 2020;78:153313.
[39] Schooling CM, Kodali H, Li S, Borrell LN. ET (Endothelin)-1 and ischemic heart disease: a mendelian randomization study. Circ Genom Precis Med 2018;11:e002026.
[40] Jin H, Bi R, Hu J, Xu D, Su Y, Huang M, et al. Elevated serum lactate dehydrogenase predicts unfavorable outcomes after

rt-PA thrombolysis in ischemic stroke patients. Front Neurol 2022;13:816216.
[41] Riviere JE, Gabrielsson J, Fink M, Mochel J. Mathematical modeling and simulation in animal health. Part I: moving beyond pharmacokinetics. J Vet Pharmacol Therapeut 2016; 39:213−23.
[42] Ki S. A semi-compartmental model describing the pharmacokinetic-pharmacodynamic relationship. Anesthesiol Pain Med 2020;15:1−7.
[43] Huang P, Tang Y, Li C, Zhou H, Yu L, Wan H, et al. Correlation study between the pharmacokinetics of seven main active ingredients of Mahuang decoction and its pharmacodynamics in asthmatic rats. J Pharm Biomed Anal 2020;183: 113144.
[44] Louizos C, Yáñez JA, Forrest ML, Davies NM. Understanding the hysteresis loop conundrum in pharmacokinetic/ pharmacodynamic relationships. J Pharm Pharmaceut Sci 2014;17:34−91.